

**ASSEMBLING PRIMITIVE CELLS UNDER MARTIAN
GEOCHEMICAL CONDITIONS:**

*Implications for the Origin and Survivability of Life
on Early Mars*

A THESIS SUBMITTED TO THE GRADUATE DIVISION OF THE UNIVERSITY OF
HAWAI‘I AT MĀNOA IN PARTIAL FULFILLMENT OF THE REQUIREMENTS FOR THE
DEGREE OF MASTER OF SCIENCE
IN
EARTH AND PLANETARY SCIENCE

NOVEMBER 2022

By

Francesca Cary

Thesis committee:

Sarah Fagents

Kathleen Ruttenberg

Joseph Jarrett

In collaboration with:

David Deamer

Bruce Damer

Keywords: astrobiology, origin of life, protocells, early Earth, Mars, iron, selection,
hydrothermal, prebiotic chemistry

Acknowledgments

This endeavor would not have been possible without collaboration with Prof. David Deamer and Dr. Bruce Damer at UC Santa Cruz, and the BIOTA Institute. They provided mentorship, academic support, and funding for all my experiments, which otherwise would not have been attainable for the chosen thesis topic.

I would like to express a deep appreciation of Dr. Sarah Fagents for supporting me in pursuing the research most aligned with my goals, and for providing me with the opportunity to work as a student on the Mars 2020 mission, the motivation for this and ongoing research on the future exploration of Mars.

I would like to extend sincere gratitude to Prof. Stuart Donachie and Christy Handel at the Donachie Lab (Life Sciences UH) for hosting my experiments, assisting me in laboratory set-up, and maintaining sanity.

I am also incredibly grateful to have had Prof. Joseph Jarrett and Prof. Kathleen Ruttenberg on my committee, for their depth of knowledge, open minds, encouragement, and continued support for my laboratory work throughout my research.

I would not be here without the generous support of the Australian-American Fulbright Association, who provided me with full funding throughout my entire master's program.

And lastly, a special thanks to Matthew Baldes, for being a supportive and knowledgeable sounding board during the critical early moments of idea synthesis, and for always guiding me towards feasible and meaningful goals beyond what I ever imagined possible before.

Abstract

Mars has been a focus for decades of investigation, as a place in the solar system that could have been habitable for life as we know it. Despite being habitable early in its history, it is important to consider whether Mars could have *originated* life; a necessary foundation for understanding whether life could have inhabited Mars. Little work has been done to directly apply current knowledge about the origin of life to the unique conditions and planetary history of Mars. This research aims to take into account broad geochemical differences between Mars and Earth, such as Mars' iron-rich surface, and assess how conducive early Mars was to originating life. Iron, calcium, and magnesium cations are abundant in hydrothermal settings on both Earth and Mars, which constitute promising environments for life's origin. The impacts of different ionic compositions on the assembly, stability, and destruction of primitive cells have been investigated for this thesis. Additionally, we investigate other components in ancient hydrothermal settings that could have increased the stability and survivability of primitive cells. We find that iron destabilizes primitive cell membrane formation less than does calcium. The concentrations of cations required to completely destabilize primitive membranes are higher than those found in natural settings on Earth, but could potentially have reached these high concentrations on Mars as a consequence of the loss of surface water. In addition, dehydration-rehydration cycles of primitive membranes in the presence of RNA stabilize them against cations in solution. High concentrations of cations in solution thus could have functioned as a significant selective barrier on Mars. Interaction of membrane vesicles and functional polymers, which stabilize primitive cells against changes in the environment, could have been a mitigating factor. This work initiates an avenue of Mars astrobiology research that considers how cellular life may have evolved under the distinct planetary conditions and selective factors on Mars.

Plain-language summary

‘How life began’ is one of the most challenging questions we pose in our efforts to search for life on other planets, such as Mars. Although Mars and Earth had similar conditions early in their histories, there are meaningful differences between the two planets that could have affected life’s beginnings. This research aims to investigate how broad differences in the geology and chemistry on Mars, as contrasted with Earth, could have affected the process of forming cellular life in a location hypothesized for life’s origin on Earth, volcanic hot springs. This research explores how the chemical conditions of martian hot springs could have affected the formation of primitive versions of cellular life, and explores the challenges life on Mars may have faced. This helps us understand how life may have taken a different evolutionary path on Mars, which is relevant to forming strategies for future exploration missions seeking signs of ancient life on Mars.

Table of Contents

1. Introduction	1
2. Background	5
2.1 Where did life start on Earth? An introduction to the hot spring hypothesis for an origin of life on Earth	5
2.2 Where could life have started on Mars? A comparison of hydrothermal settings on Mars	8
2.3 How did life emerge from chemistry? Understanding natural selection and the evolutionary processes that preceded biology	9
2.3.1 Review of Natural Selection	9
2.3.2 Pre-Darwinian selection	10
2.4 What are the chemical properties of lipids and protocells? Bioorganic chemistry relevant to protocell formation, aggregation, and wet-dry polymerization	12
2.5 How do we know Mars has more iron at the surface than Earth?	13
2.5.1 How are metal cations mobilized from rocks? An explanation of how planetary oxidation state impacts chemical weathering and cation liberation.	15
2.6 Why has iron been readily utilized by biology?	16
3. Experimental approach	17
3.1 Rationale	17
3.2 Justification for key experimental parameters and variables	18
3.2.1 Working with ferrous iron	18
3.2.2 Choice of Fe ²⁺ source	19
3.2.3 pH Conditions	20
3.2.4 Choice of buffers	20
3.2.5 Choice of nucleic acid	20
3.2.6 Why investigate protocell aggregation?	21
4. Methods	21
4.1. Aggregation of lipid vesicles in the presence of cations	25
4.2. Aggregation of lipid vesicles with encapsulated RNA in the presence of cations	26
4.3 Note on uncertainty, replicates, and natural variability of data	27
5. Results	28

5.1 Microscopy	28
5.2 Iron oxidation state in solution	29
5.3 Lipid vesicle aggregation with calcium, iron, and magnesium	30
5.3.1 Lipid vesicles in neutral and acidic pH	32
5.3.2 Lipid vesicles made of LAGML and CAGML	33
5.3.3 Lipid vesicles made of LA and LACA	34
5.3.4 Lipid vesicles made of LAGML and RNA	35
5.4 Temperature and aggregation (preliminary observations)	36
5.5 Summary of results	37
6. Discussion	37
6.1 Role of atomic properties on cation-induced vesicle aggregation	37
6.1.1 Role of Mg ²⁺ in protocell evolution?	41
6.2 Environmental effects on vesicle aggregation	41
6.2.1 Effect of pH on vesicle formation	41
6.2.2 Effect of temperature on aggregation	43
6.3 Effect of fatty acid composition	44
6.3.1 Effect of carbon chain length and temperature on lipid vesicle formation	44
6.3.2 Effect of mixed fatty acid ‘mosaic’ vesicles	45
6.4 Concentration of cations in natural settings	47
6.5 Role of RNA in protocell evolution	49
6.5.1 RNA-fatty acid interaction during wet-dry cycling	49
6.5.2 Multilamellar vesicles	51
6.5.3 Effect of morphological differences on light absorbance	51
6.5.4 Selection on the interaction between RNA and lipid vesicles.	52
6.6 Role of iron in protocell formation	53
6.7 Research context	54
7. Implications and Conclusions	55
7.1 Future work	55
7.2 An origin of life on Mars: Strategizing where we search for life based on the additional environmental challenges on Mars	58
7.3 Concluding remarks	61

References	63
Appendices	72

List of Tables

Table 1: Vesicle preparation reference key.	25
Table 2: Summary of the atomic properties of calcium, iron, and magnesium that affect interactions with fatty acids and water.....	72
Table 3: Previous investigations of conditions for protocell formation and aggregation that this thesis research builds from, highlighting novel findings.	7254
Appendix 1 , Table 1: Vesicle preparation reference key (repeated), where lipids were prepared for aggregation experimentation to make vesicles composed of various mixtures of lauric acid (LA), capric acid (CA), glycerol monolaurate (GML), and RNA in buffer.	75

List of Figures

Figure 1: Micrograph of fatty acid vesicle formation.....	1
Figure 2: Uorable factors on Mars supporting the formation of protocells over time.....	3
Figure 3: Summary of the Hot Spring Hypothesis for an origin of life.....	7
Figure 4: Chemical structures of membrane lipids, micelles and vesicles, as well as the metal cation-lipid binding interaction.....	12
Figure 5: Condensation reactions and polymer formation.....	13
Figure 6: Controlled atmosphere chamber set up for anaerobic conditions and experimentation under nitrogen gas.....	19
Figure 7: Fatty acid vesicle solution increasing in turbidity with addition of Ca ²⁺ cations	22
Figure 8: Micrographs of lipid vesicles aggregating in the presence of Ca ²⁺ , both with and without a wet-dry cycle, as well as with encapsulated RNA.....	23
Figure 9: RNA encapsulated and concentrated inside LAGML vesicles	27
Figure 10: Light absorbance of LAGML lipid vesicle solutions with increasing concentrations of ferrous and ferric iron.....	30
Figure 11: Increasing absorbance (aggregation) with increasing concentration of calcium, iron, and magnesium cations.....	31

Figure 12: Light absorbance of LAGML lipid vesicle solutions with increasing cation concentrations, pH 7.5 and pH 5.5.....	72
Figure 13: Light absorbance of LAGML and CAGML lipid vesicle solutions with increasing cation concentrations, pH 7.5	72
Figure 14: Light absorbance of LA and LACA lipid vesicle solutions with increasing cation concentrations, pH 7.5.....	72
Figure 15: Light absorbance of LAGML and RNA-LAGML lipid vesicle solutions with increasing cation concentrations, pH 7.5	72
Figure 16: Average light absorbance of lipid vesicle solutions with temperature.....	72
Figure 17: Physical interactions between lipid vesicles at 20°C and 50°C.....	72
Figure 18: Modern biology contains echoes of prebiotic chemistry e.g. 'hybrid vigor'.....	46
Figure 19: Cation concentrations for calcium, magnesium, and iron observed to produce aggregation in this study compared with natural hot spring settings.....	72
Figure 20: 'Wet-dry' cycles in natural hot spring pools generates three phases of lipid vesicle encapsulation: wet (vesicles and protocells), intermediate (lipid-polymer gel) and dry (concentrated lamellar film of fused lipids)	72
Figure 21: Light absorbance of LAGML lipid vesicle solutions in near-neutral pH (7.5) with increasing cation concentrations	78
Figure 22: Light absorbance of LAGML lipid vesicle solutions in acidic pH (5.5) with increasing cation concentrations	79
Figure 23: Light absorbance of CAGML lipid vesicle solutions with increasing cation concentrations, pH 7.5	80
Figure 24: Light absorbance of LA lipid vesicle solutions with increasing cation concentrations, pH 7.5	81
Figure 25: Light absorbance of LA lipid vesicle solutions with increasing cation concentrations, pH 7.5	82
Figure 26: Light absorbance of RNA-LAGML lipid vesicle solutions with increasing cation concentrations, pH 7.5.....	83
Figure 27: LAGML vesicles immediately after exposure to salt water and the ionic composition of hydrothermal and seawater comparatively.	84
Figure 28: Spectrophotometer scans of LAGML-cation samples, demonstrating maximum light transmission at ~ 400 nm.....	85

1. Introduction

The assembly of cellular life on Earth required the formation of membranous boundary compartments, a requirement that is evident in modern organisms as an echo of primitive versions of cellular life. Membrane-forming compounds such as fatty acids are readily available through meteorite infall and geochemical synthesis in hot spring settings (McCollom et al., 1999; Deamer & Dworkin, 2005; Rushdi & Simoneit, 2006; Damer & Deamer, 2020). Fatty acids can self-assemble into vesicles (Figure 1) because they possess both hydrophilic and hydrophobic properties (Section 2.4) and can encapsulate geochemically synthesized nucleic acids and polymers thought to be precursors for RNA. The resulting structure is referred to as a protocell, which can aggregate into proto-cellular networks that are collectively capable of primitive, pre-



Figure 1: Micrograph of fatty acid vesicle formation under the microscope at 40X magnification. Vesicles are made of lauric acid and glycerol monolaurate in water and buffer (TEA, pH 7.5).

Darwinian evolution (Damer & Deamer, 2020). Protocells represent the earliest structures of life on Earth, and potentially on other rocky water-bearing worlds such as Mars.

Previous astrobiological investigations of Mars largely focused on habitability, projecting what we know about the timescale of life's emergence on Earth to Mars, and drawing similarities between their potential to host life. Given the broad similarities between Mars and Earth, extrapolation to Mars of the conditions that we know contributed to the origin of life on Earth is reasonable to some degree. The complex set of environmental conditions involved in creating an origin of life opportunity are described as 'urable' properties (Deamer, Cary & Damer, 2022), and early Mars shared many urable properties with Earth, and thus a comparable urability. Both planets display evidence of volcanic landscapes and liquid water seas early in their histories, with similar availability of light energy, anoxic atmospheres, and organic compounds (either delivered during late accretion or synthesized by atmospheric or geochemical reactions). Additionally, both planets had a dynamic surface environment capable of driving chemical evolution, such as a hydrological cycle that produced evaporation and precipitation in diverse chemical conditions on volcanic hot spring landscapes. Given that these key factors are shared with the prebiotic chemistry of the early Earth, it is reasonable to think that Mars had the opportunity to support the origin of life processes for assembling primitive cells to some degree. However, little work has been done to directly apply our current hypotheses for an origin of life to the different conditions on Mars, which could have meaningfully impacted whether life could have begun the same way on Mars as it did on Earth. The urable factors contributing to the formation of protocells on Mars (Fig. 2) indicate that the changing surface conditions could have adversely impacted protocell-forming processes on early Mars. This thesis research focuses on the effect of metal cation concentration on protocell formation on Mars.

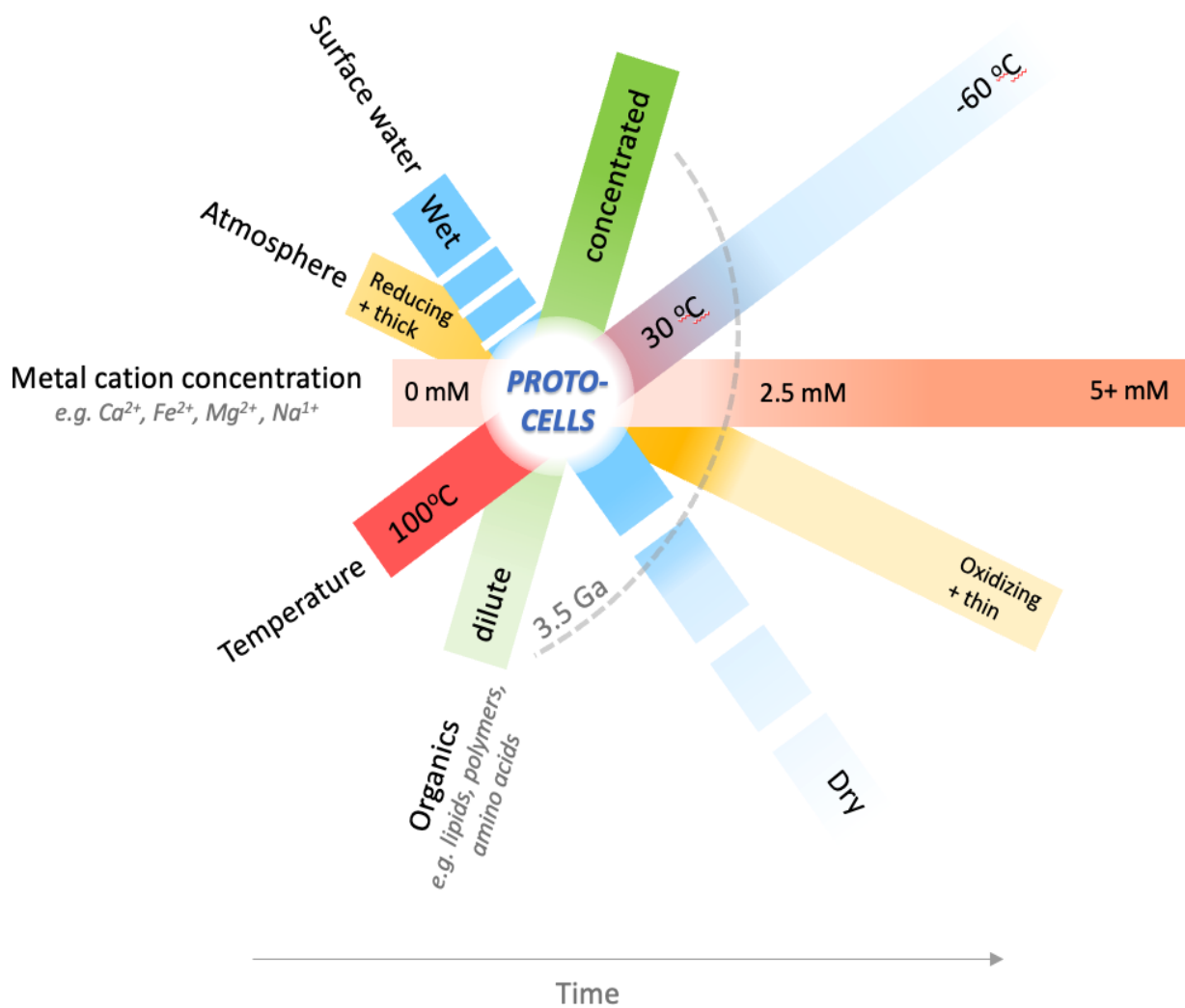


Figure 2: Schematic composed of overlapping bars representing urable factors on Mars that could support the formation of protocells and, if conditions persisted long enough, could favor the evolution of protocells into living cells. The abrupt shift in planetary conditions at ~ 3.5 Ga, depicted as a gray dashed curve, represents the coinciding change in atmospheric, hydrological and geochemical conditions that would have made protocell formation on Mars more challenging beyond 3.5 Ga. If protocells or early living cells had acquired the molecular machinery to adapt to these changing surface conditions, they may have survived this shift. However, the dramatic change over a relatively short period of time (~ 200 million years or so) would have been a significant adaptive challenge even for well-established life on Mars. The white lines on the bar representing surface water indicate cycles of hydrated and dehydrated conditions, including short-term (hours, days, or weeks) wet-dry cycling and long-term cycling during episodic surface water (years, thousands of years, or millions of years). Urability graph adapted from Deamer et al., 2022.

Ancient hot spring deposits have been identified on Mars that date to a corresponding period in Earth's formation history when cellular life was thought to have emerged in such environments (Michalski et al., 2017; Sasselov et al., 2020). However, the two planets have diverged in terms of their surface conditions over the past 4 billion years, and there are meaningful geochemical differences to consider when considering environmental impacts on the origin of life. Little is known about the effect of specific geologic and chemical differences on the process of protocell formation under early martian versus early terrestrial conditions. Investigating different geochemical conditions for protocell assembly could establish an understanding of how hot spring settings on early Mars compared to Earth in their ability to facilitate the assembly of cellular life.

One globally evident difference between Mars and Earth is the higher iron content in the crustal minerals of Mars (Stevenson, 2001; Zuber, 2001; Halliday et al., 2001; Taylor et al., 2009), supported by observations of surface geology on Mars through remote sensing, and in situ rover and lander exploration (e.g., Gellert et al., 2004), as well as by martian meteorite samples. Ferrous iron (Fe^{2+}) is thought to have dominated early Mars before oxidizing to ferric (Fe^{3+}) iron (Dehouck et al., 2016; Liu et al., 2021), and dissolved cations, including iron, have important implications for the self-assembly of lipid vesicles and protocells. For example, fatty acids contain charged hydrophilic carboxylate groups ($-\text{CO}_2^-$), so vesicles with membranes made of fatty acids are sensitive to collapse in the presence of divalent cations such as Ca^{2+} and Mg^{2+} (Deamer & Dworkin, 2005; section 2.3), and potentially Fe^{2+} as well.

Iron is known to play a key role in biological functions such as metabolism and enzyme activity, and in a primitive world Fe^{2+} preceded the role of Mg^{2+} in catalyzing RNA synthesis in anoxic environments (Hsiao et al., 2013; Okafor et al., 2017; Guth-Metzler et al., 2020). Dissolved ferrous iron was additionally thought to have been present in the Archean oceans at high

concentrations before the Great Oxidation Event (GOE) (Rouxel et al. 2005). Given that protocell membranes are likely to be sensitive to iron cations as they are to calcium and magnesium cations, early life on Mars would have needed to overcome this sensitivity. If protocells on Mars developed mechanisms to maintain robust membranes in the face of iron cations, perhaps the high iron content could have then been utilized by emerging proto-cellular networks in catalyzing biological chemistry, such as polymer formation. *Understanding the relationship between geochemistry and keystone organic molecules in protocell assembly processes, and in catalyzing biological chemistry, is relevant to relating the different environmental conditions of Mars and Earth to the origin of life.*

2. Background

2.1 Where did life start on Earth? An introduction to the hot spring hypothesis for an origin of life on Earth

Ultimately, life emerged from chemistry, and the local chemistry is determined by planetary and geologic context. This connection between the chemical environment and the life that emerges from it has contributed to the formation of two alternate hypotheses for environments favorable to the origin of life on Earth: deep-sea hydrothermal vents and volcanic hydrothermal hot springs on land. Both hypotheses explain the formation of ‘prebiotic geochemistry’, the chemical conditions and compositions of organic molecules resembling those incorporated into life we see today (such as amino acids, lipids, polymers, RNA precursors, metal catalysts, etc.), but have different focuses in relation to the processes of life’s emergence. The deep-sea vent hypothesis focuses on the synthesis of prebiotic molecules and the formation of energy gradients. This hypothesis has dominated origin of life research in past decades, but is now subject to criticism for the following

reasons: salty seawater is destructive to fragile cell membranes and emerging protocell networks; the enormous volume of the ocean's water dilutes organics or the protocells formed; the distance from the bottom of the ocean to land is a great barrier for development of photosynthetic life under the timescales expected for Earth (~3.5 Ga, Blankenship, 2010); and there is an absence of polymer-formation mechanisms such as wet-dry cycling and condensation reactions (section 2.4) that are observed in subaerial landscapes that interact with Earth's atmosphere. In contrast, the hot spring hypothesis is focused on the *combinatorial* aspect of the origin of life, rather than organic molecule synthesis and energy availability. Volcanic hydrothermal landscapes can drive the concentration and combination of molecular ingredients into protocells. The formation of protocells is driven by a dynamic environment that facilitates cycles of hydration and evaporation, as well as fluctuating chemical conditions. A surface hydrothermal environment such as hot spring pools can provide this dynamic environment, as well as selective factors which in combination drive evolutionary processes and a pre-Darwinian style of selection on protocells (Figure 2).

It is important to note that prebiotic chemistry does not mean that life has begun, rather it means that the right ingredients are available to make life as we know it, but a system for combining these ingredients into an interacting whole is required for life to form. The hot spring hypothesis was selected as the theoretical framework for this research as it provides a more dynamic, combinatorial, and diverse landscape, which is the foundation for driving selection and the evolution of chemicals to become part of a broader living system.

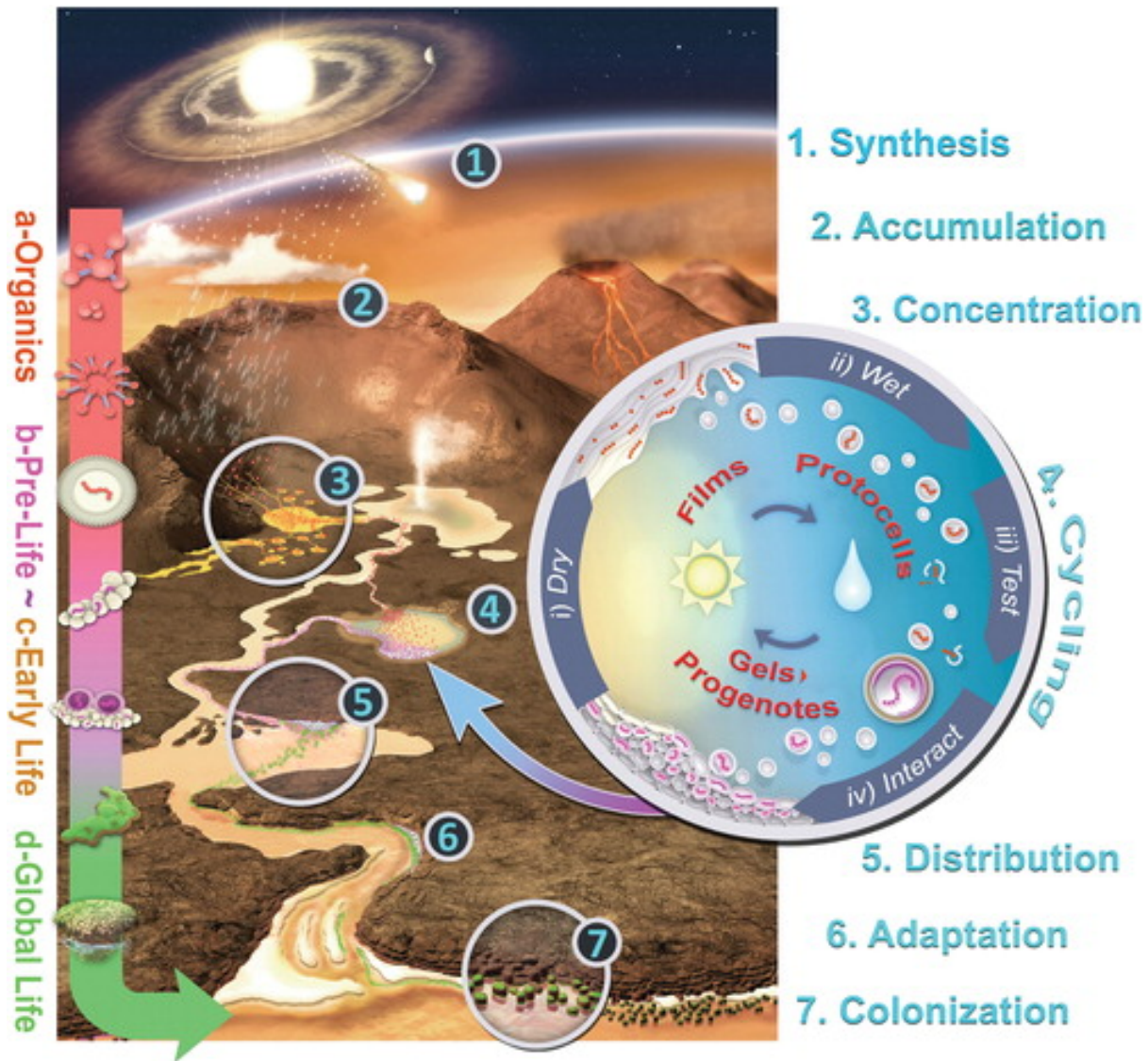


Figure 3: Summary of the Hot Spring Hypothesis for an origin of life, from Damer & Deamer (2020). Volcanic hydrothermal hot spring landscapes on Earth ~ 4 Ga could have facilitated the formation and evolution of prebiotic chemistry on the path to becoming cellular life. These settings are capable of synthesizing and accumulating organics that compose protocells, as well as concentrating and combining them into protocells inside hot spring pools. Hot springs dry out and rehydrate during natural precipitation cycles, and when protocells dry down, polymer transfer can take place as protocells fuse their membranes in a multilamellar structure. Upon rehydration, diverse populations of protocells regenerate and bud off from the multilamellar lipid matrix, and are subjected to selective pressures from the environment. Networks of hot spring pools with diverse chemical conditions provide selective barriers for protocell communities as they are transported between pools, providing an opportunity for continuous adaptation towards inhabiting new niches on the surface of the early Earth.

2.2 Where could life have started on Mars? A comparison of hydrothermal settings on Mars

A hot spring setting hypothesized for an origin of life on Earth is also a favorable environment for life's origins on Mars. Various volcanic hydrothermal sites have been identified on Mars (Michalski et al., 2017; Sasselov et al., 2020; Longo & Damer, 2020), but seafloor vents have yet to be conclusively discovered in the martian northern hemisphere, where it is possible an ocean could have formed (Longo & Damer, 2020). Additionally, Mars lacks plate tectonics, a geologic process that drives the formation of deep-sea hydrothermal vents (Fornari & Embley, 2013). Some might argue that hydrothermal vents can still be formed at magmatic hotspots on Mars (Langmuir et al., 1997), and thus perhaps a hydrothermal vent scenario could have originated life there. However, these settings represent a minority of hydrothermal settings on Mars compared to the widespread subaerial hydrothermal settings (Longo & Damer, 2020). If deep-sea vents were less common than subaerial hydrothermal systems on Mars, this reduces their plausibility as a robust origin of life environment, given that an origin of life transition has to occur on a planetary scale (Furukawa & Walker, 2018; Sasselov et al., 2020; Frank, Grinspoon & Walker, 2022) rather than occurring in any one isolated pocket of a planet. Therefore, there is reason to believe that deep-sea vents would not have been the dominant hydrothermal activity on Mars. Instead, volcanic hot springs are more likely as sites for origin of life processes in hydrothermal settings.

Land-based hydrothermal settings on Mars can be divided into two categories, 1) volcanic and 2) impact-generated. Mars had widespread volcanism and a hydrosphere capable of creating hot spring pools, but impact-generated hydrothermal pools were also present on the surface of Mars (Abramov & Kring, 2005). If impact-driven hydrothermal pools dominated the surface of Mars, they may not have been ideal sites for sustaining the relevant chemical processes. For

example, they lack volcanic gas emissions which drive chemical diversity mechanisms such as fluctuations in pH, in addition to having relatively short-lived sources of heat driving hydrothermal activity, two important favorable factors in these settings (Deamer et al., 2022). Impact-driven hydrothermal sites may however become habitable paleolakes (Abramov & Kring, 2005), but similarly to the drawback with a deep-sea origin of life, paleolakes would be too large and dilute for chemical processes and abiogenesis to occur comparably to smaller hot spring pools (Longo & Damer, 2020). However, there was no shortage of volcanic activity on Mars, and hot springs would likely have been present in sufficient abundance to facilitate processes similar to on Earth (described above: section 2.1), and thus represent a plausible site for an origin of life on Mars.

2.3 How did life emerge from chemistry? Understanding natural selection and the evolutionary processes that preceded biology

Before biology, the underlying processes of selection and evolution applied to molecules on a chemical level. Conceptually, the evolution of a system can take place when there is 1) continuous variability in the components of the system, 2) interaction of the components with the environment of the system 3) destruction or removal of some constituents from the system while others persist and propagate, and 4) a mechanism that *selects* among the constituents and determines whether the constituent persists or perishes (Cohen and Marron, 2020). This selection mechanism is critical to the evolution of the system and need not be specific to the type of system it is acting upon. It is helpful to consider selection at the chemical level when assessing what processes were involved in the transition from abiotic to living chemistry.

2.3.1 Review of Natural Selection

We are most familiar with the concept of selection in Darwinian evolution, where the mechanism for evolution of life on Earth is natural selection. This selection mechanism fulfills the criteria (1-

4) listed above and applies best at the level of a multicellular organism or populations of organisms within a species. In natural selection, there is diversity in the characteristics between organisms within the same species that is generated spontaneously (1). These characteristics are selected by nature based on the effect they have on the survival and reproduction of the organism relative to the others within the same species in the environment (2, 4). These characteristics get passed on genetically to the offspring (3), and thus the effect of selection over generations is referred to as evolution. Modified versions of selection can apply to multiple scales of biology beyond the species level, from individual cells up to ecosystems and even the biosphere as a whole, including cultural products such as society and technology. However, the mechanisms driving selection vary among these scales of life, and it is necessary to consider the mechanisms for selection most relevant at the interface between chemistry and life at life's origin.

2.3.2 Pre-Darwinian selection

The principles of evolution facilitated by selection apply to scales deeper than life, and chemical systems can evolve in a pre-Darwinian fashion at the scale of molecules (Damer & Deamer, 2020), which was a driving force of life's origins. Molecules can be selected by the environment based initially on their *physical stability* (what gets to exist), and in the case of living chemistry, molecules can transition to being selected based on their *function and behavior* within that chemical system and molecular network (how existence is amplified). Over time and chemical cycles — chemistry's version of 'generations' (3) — degradation and new interactions proceed and certain molecules become better suited than others to exist in a certain chemical environment, which provides the foundation for subsequent modifications, feedback loops, and construction of more complex structures, including robust macrostructures such as protocells.

An example of selection at the chemical level that was relevant to prebiotic chemistry is the transition from simple lipids found prebiotically in meteorites (e.g., lauric acid $C_{12}H_{24}O_2$) to the membranes found in modern cells (e.g., phospholipids $C_{39}H_{75}O_{10}P$), as indicated in Deamer & Dworkin (2005). The first cells were made of simple lipids which formed membranous vesicles, which are spherical hollow aggregations of lipids which self-assemble in solution. Over time early cells developed membrane vesicles better suited to prolonged survival in the environment. This included having multiple (and longer) carbon-chain tails, mixed fatty acid compositions (observed in this research and described in section 6.3.2), and a phosphate group. This is an example of chemical selection based on physical stability, where the phosphate group and mixed fatty acid composition of membranes helped stabilize vesicles and allow them to develop novel functions later.

A transition from *passive* physical stability to *functional* physical stability is a key aspect of chemical selection in the origin of life. For example, the inclusion of RNA inside vesicles stabilizes them in a changing environment (sections 5.3.4 and 6.5). The interaction between RNA and lipid vesicles (evolutionary criterion 4) is ‘cooperative’ to enhance the survivability and propagation of the resulting combined structure (Damer & Deamer, 2020). The selection process that produces robust interactions between molecules that have *functional* physical stability is driven by the chemical environment during the origin of life. Cooperation for robustness at the chemical level is also conserved at the biological level, where bacteria tend to collaborate more than compete for their survival tracing back to their origin of being selected based upon how well they could passively collaborate in order to exist physically (Damer and Deamer, 2020).

To summarize, selective factors allowed chemicals on the prebiotic Earth to become organized into a collaborating and self-perpetuating system capable of evolution. Natural selection

is an echo of an underlying selection mechanism in the universe that applies to multiple scales of phenomena, and serves as a base framework to abstract when applied to systems precursory to biology.

2.4 What are the chemical properties of lipids and protocells? Bioorganic chemistry relevant to protocell formation, aggregation, and wet-dry polymerization

Lipids that form membranes in cells and protocells are a class of molecules called ‘amphiphiles’, meaning one side is hydrophilic (attracts water) and the other is hydrophobic (repels water). This chemical property allows for the *spontaneous self-assembly* of lipids into bilayers resulting in vesicles with encapsulated water and other contents in their interiors (a structure ready to become a protocell). Alternatively, micelles can form which do not capture any content as the hydrophobic chains associate with each other instead of forming a bilayer (Figure 4).

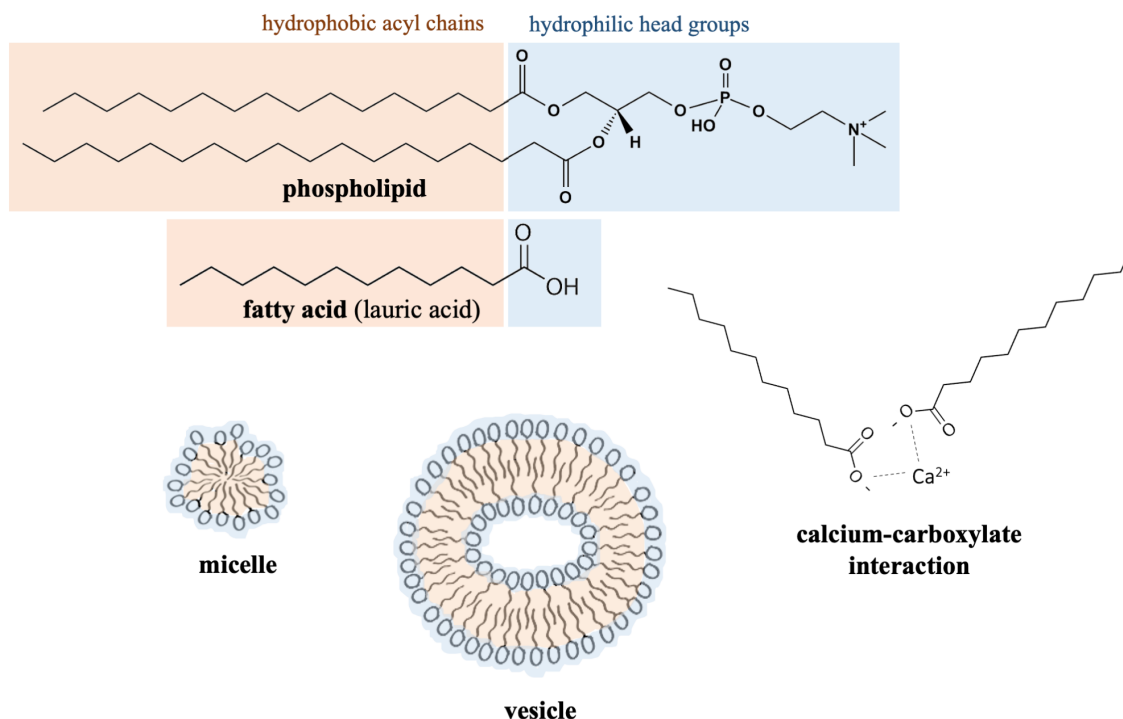


Figure 4: Chemical structures of membrane lipids (phospholipids and fatty acids), cartoons of their self-assembly into micelles and vesicles, as well as the interaction between metal cations and the hydrophilic head group of lipids.

The hydrophilic head group of fatty acids are negatively charged anion sites made of carboxylate groups ($-\text{CO}_2^-$), which can bind with positively charged cations such as metal ions (e.g., Ca^{2+}). Metal cations can form multiple coordinate bonds with these carboxylate groups and 'bridge' fatty acids, which causes a physical effect on a macro-molecular scale known as 'aggregation' or 'flocculation' (Black et al., 2013). Here, fatty acids form clusters of metal cation-lipids instead of membranous vesicles capable of becoming protocells and participating further in the system. *Metal cations are common in hydrothermal settings and have the capability to completely destabilize vesicles. Therefore, vesicles with properties that make them robust in the face of cations have a selective advantage during the emergence of cellular life.*

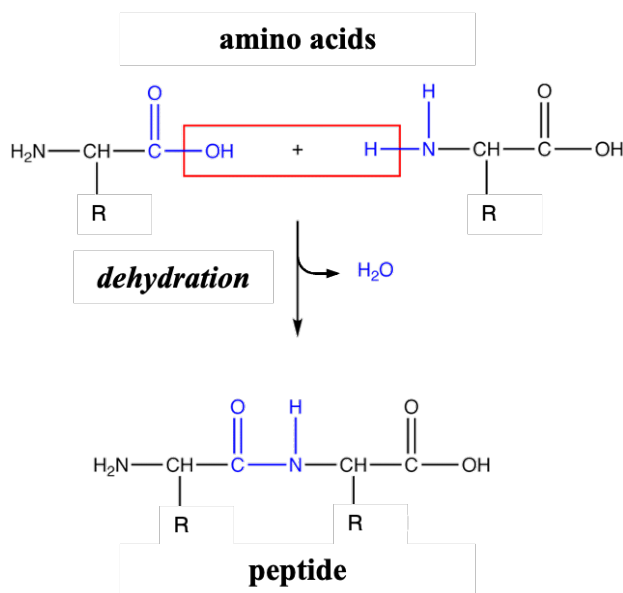


Figure 5: Condensation reactions that link individual amino acids into polymers (peptides) as a result of a dehydration reaction.

2.5 How do we know Mars has more iron at the surface than Earth?

Mars has a high surface expression of iron relative to Earth (Zuber, 2001) which indicates a different planetary differentiation history. Mars' reduced size, gravity, and more rapid cooling history left a greater abundance of FeO in the mantle, because less iron was able to sink into the core over the shorter timescale for chemical differentiation (Halliday et al., 2001). The broad effect

of this on surface geology is a higher relative abundance of iron in basaltic volcanic deposits, which is significant because volcanic lithologies host hydrothermal hot springs.

Gusev crater on Mars, explored by the Spirit rover, has evidence of a volcanic hydrothermal system in a site known as Columbia Hills (Ruff et al., 2020). Opaline silica sinter deposits have been identified at this site with morphologies consistent with biologically mediated hydrothermal hot spring deposits on Earth, such as El Tatio in Chile (Ruff et al., 2020; Van Kranendonk et al., 2021). Overall, analysis of the average volcanic basalts in Gusev crater indicate a high weight percentage of FeO, followed by Al₂O₃, MgO, and CaO (Gellert et al., 2004). The total molar composition of iron in Gusev crater rocks is similar to Earth basalts (~0.84-90) (McSween et al., 2004), but the abundance of iron relative to calcium reflects a high iron content and more ultramafic composition on Mars, e.g. ~ 20 wt. % Fe and Mg oxides and < 2 wt. % Ca oxides, as identified by Spirit in Comanche Spur Palomino (Gellert et al., 2004). The high weight percentage of FeO found in Gusev is also similar to abundances at the Viking and Pathfinder landing sites, and comparable with primitive ultramafic Archean rocks on Earth (komatiites; Gellert et al., 2004).

Inevitably there is a limited regional context and sample selection for basalts on Mars relative to Earth, and the exact iron content of landing sites is subject to sampling bias for crater lakes over volcanic remnants in the martian highlands. Despite this, a robust global trend of high iron content is evident (Stevenson, 2001; Zuber, 2001; Halliday et al., 2001; Taylor & McLennan, 2009), and arguably more valuable for understanding the implications for an origin of life on Mars, because life did not emerge only in isolated discrete locations but rather in a networked landscape as a broader planetary scale process that encompasses many localized settings (Sasselov et al., 2020).

2.5.1 How are metal cations mobilized from rocks? An explanation of how planetary oxidation state impacts chemical weathering and cation liberation.

Iron at the surface of Mars transitioned from ferrous (Fe^{2+}) to ferric (Fe^{3+}) in an abiotic ‘Great Oxidation Event’ as the planetary scale redox chemistry changed in the late Noachian due to atmospheric escape and increased UV radiation exposure (Liu et al., 2021), but early Mars is thought to have had a reducing atmosphere, as evident in the rock record. For example, Fe^{2+} -rich clay minerals have been detected in Noachian pelagic sediments derived from aqueous hydrothermal deposits (Michalski et al., 2017). Under a reducing early Mars atmosphere, anoxic and acidic chemical weathering would mobilize Fe^{2+} from rocks such that it would accumulate in fluids (Liu et al., 2021), preferentially leaving behind aluminum, which is comparable in abundance to iron on Mars (McSween et al., 2004; Gellert et al., 2004). Such chemical weathering can mobilize the dominant cations found in present day hydrothermal solutions (calcium, magnesium, and iron) and occur in the absence of free oxygen, which is representative of hydrothermal solutions early in Earth and Mars’ histories. For example, under weakly acidic conditions, calcium-bearing minerals such as calcite can undergo dissolution and have their calcium mobilized as Ca^{2+} divalent cations ($\text{CaCO}_3 + \text{H}^+ + \text{HCO}_3^- \rightarrow \text{Ca}^{2+} + 2\text{HCO}_3^-$). Similarly, iron-bearing minerals such as olivine undergo dissolution in the presence of carbonic acid, and can mobilize the iron as Fe^{2+} divalent cations ($\text{Fe}_2\text{SiO}_4 + 4\text{H}_2\text{CO}_3 \rightarrow 2\text{Fe}^{2+} + 4\text{HCO}_3^- + \text{H}_4\text{SiO}_4$) (Earle, 2020). Both of these reactions proceed without O_2 . These are examples of how cations can become mobilized to participate in hydrothermal chemistry plausible for reducing conditions on early Mars and Earth.

2.6 Why has iron been readily utilized by biology?

Life on Earth uses specific elements for biochemistry, but there is no clear understanding of what governs the choice of elements used by life. Perhaps the selection of specific elements for life can be partially explained by considering a combination of local availability and chemical usefulness in the environment of life's origin and evolution.

Iron has had a unique impact on biology because of its extreme redox sensitivity. Iron's capacity to liberate electrons makes it a useful catalyst, but also makes it very susceptible to oxidation. Earth's atmosphere converted to oxidizing conditions during the Great Oxidation Event GOE, giving iron a dual nature in biology, contributing both advantageous and detrimental effects on life (Kaplan & Ward, 2013). The resulting impact on biology is that life has conserved its ability to sequester iron and regulate its concentration inside cells, but has also become adept at dealing with the toxicity of oxidized iron. For example, protein-based metal ion transporters that control iron transfer into and out of cells (e.g., DMT1/NRAMP1 and Mrs/mitoferrin transporters) and enzymes that synthesize iron-containing cofactors have both been conserved through evolution (Kaplan & Ward, 2013). This indicates that iron played an essential role in early biological activity, which is further supported by its other contributions to biological chemistry, such as expanding the catalytic repertoire of RNA (Hsiao et al., 2013), acting as an ideal redox active cofactor (Outten & Theil, 2009), and catalyzing RNA (Okafor et al., 2017), amino acids (Barge et al., 2019), and other organic compound (Deamer & Dworkin, 2005) synthesis (Kaplan & Ward, 2013).

3. Experimental approach

3.1 Rationale

The first step toward understanding how iron-rich martian geochemistry affects protocell formation is to quantitatively investigate the relative effect of Fe^{2+} compared to other cations with established effects on lipid vesicles, such as Mg^{2+} and Ca^{2+} (Milshteyn et al., 2018; Deamer et al., 2019). Building on the previously successful and widely implemented experiments by Prof. David Deamer, such as the Milshteyn et al. (2018) study on protocell assembly in hot spring and seawater solutions, the present study investigates the assembly and stability of protocells in the presence of the dominant cations found in hot springs. Experiments first compare the effect of Fe^{2+} , Ca^{2+} and Mg^{2+} on vesicle self-assembly and stability, using increased abundance of iron as a plausible key difference in the ionic composition of hydrothermal settings on Mars versus Earth. In the presence of cations, fatty acids can form large aggregates of destabilized vesicles. This is known as ‘flocculation’ or ‘aggregation’ (Black et al., 2013). Flocculation would result in fatty acids predominantly forming aggregates at high concentrations, rather than self-assembling into vesicles that can potentially become protocells and participate in prebiotic evolution at the chemical level.

Given that the presence of cations in hydrothermal systems would lead to aggregation of fatty acids, and thus no protocell formation, it is important to identify characteristics of vesicles and their environment that will increase their stability under different conditions. Fatty acid synthesis, pH, and wet-dry cycling are controlled by local geochemical and environmental conditions, in addition to which, cationic abundances may vary between Mars and Earth. Therefore, in addition to investigating the role iron plays in vesicle stability compared with other cations, this research also explores the effects that fatty acid composition, acidic conditions, and

wet-dry cycling in the presence of polymers have on protocell stability. Combined, this builds a foundation for assessing how protocell stability might differ between environments on Mars and Earth, and more broadly, how changes in the geologic and chemical environment impacts the prebiotic chemistry that emerges from it.

3.2 Justification for key experimental parameters and variables

3.2.1 Working with ferrous iron

Given that Earth and Mars had reducing rather than oxidizing atmospheres early in their planetary evolution, maintaining anaerobic conditions during experimentation with redox-sensitive ions such as iron was critical. Fe^{2+} rapidly oxidizes to Fe^{3+} under the present-day oxidizing atmosphere, and Fe^{3+} is relatively insoluble unless the conditions are acidic ($\text{pH} \leq 3$, Kaplan & Ward, 2013), in contrast to Fe^{2+} solubility which is less sensitive to pH. In preliminary experiments, Fe^{2+} was observed to oxidize in less than 10 minutes when $\text{Fe}(\text{NH}_4)_2(\text{SO}_4)_2$ was dissolved in triethanolamine (TEA) buffer (pH7.5) solutions, even after removing dissolved oxygen by boiling or bubbling nitrogen gas through the solution, and with the flow of external oxygen limited by using a screw-cap test tube. Thus, it was necessary to adopt a method that was completely anaerobic to measure iron in the ferrous rather than ferric redox state.

All sample preparation, experimentation, and analysis described in methods section 4 were performed in an anaerobic nitrogen-purged chamber (Figure 6) unless otherwise specified. As a further precaution, buffers and water were vigorously bubbled with nitrogen and sealed prior to entry into the chamber, and the seal was removed only once solutions were placed in the chamber so that during cycles of vacuuming and flushing with nitrogen, any residual oxygen gas in the flask would be removed. Solids were pre-measured for each experiment and prepared in the chamber

after anaerobic conditions had been achieved. The chamber was sealed and flushed with nitrogen gas ~ 23 times until the oxygen content was 0.0% (measured with an O_2 monitor). A spectrophotometer was placed entirely inside the chamber so that analysis of samples could take place under anaerobic conditions.

3.2.2 Choice of Fe^{2+} source

Whilst Fe^{2+} in the form of ferrous sulfate oxidized immediately in solution (see section 5.2), ferrous sulfate was chosen as the source of Fe^{2+} cations for experimentation because Fe^{2+} was shown to have a similar effect to Fe^{3+} on aggregation as described in section 5.2, as well as to reduce uncertainty of NH_4^+ cation interference in alternative Fe^{2+} solutions made of ferrous and ferric ammonium sulfate (Figure 6, section 5.2).



Figure 6: Controlled atmosphere chamber set up for anaerobic conditions and experimentation under nitrogen gas.

3.2.3 pH Conditions

Analysis of ancient rocks from lake environments at Gale crater, as explored by the Curiosity rover, suggests pH ranges from neutral to mildly acidic (Sasselov et al., 2020). Similarly, at Columbia Hills, explored by the Spirit rover, magnesium-iron carbonates were identified that formed under near-neutral pH conditions (Morris et al., 2010), as well as opaline silica deposits that are estimated to have precipitated under near-neutral to acidic conditions (depending on the temperature; Filiberto & Schwenzer, 2013). A range of pH conditions are also of interest to prebiotic chemistry because volcanic gasses bubbling through hydrothermal pools generate diversity in pH between pools (section 2.1), which can act as a chemical selection barrier for emerging protocell communities that get flushed into new pools. Experiments in this research were primarily conducted under neutral pH (7.5), but the effect of acidic conditions (pH 5.5) was also investigated (section 5.3.1) to capture the range of plausible conditions for hydrothermal and aqueous settings on early Mars.

3.2.4 Choice of buffers

To ensure metal cations were interacting with lipids as desired, it was important to choose buffers that, in addition to being within the desired pH range, also did not interact with metals. Both the triethanolamine (TEA) buffer (pH 7.5) and 2-(N-morpholino)ethanesulfonic acid (MES) buffer (pH 5.5) have negligible metal-ion binding tendencies (Calbiochem buffer preparation manual) and thus were chosen for experimentation.

3.2.5 Choice of nucleic acid

RNA (yeast extract) was chosen for experimentation. Although RNA is an evolved molecule that formed from a lineage of precursor polymers, for the purposes of observing the effect of a nucleic acid polymer on protocell formation, RNA is readily available and easy to work with. It is also

more prebiotically plausible than DNA, which is thought to have evolved from (Forterre et al., 2013) or co-evolved with RNA (Gavette et al., 2016), and represents the broad chemical behavior of nucleic acid polymers. Ribosomal (rRNA) was chosen for its shorter chain length (~100 bp) than messenger (mRNA, ~1000 bp).

3.2.6 *Why investigate protocell aggregation?*

There is extensive research on protocell formation (reviewed in Gözen et al., 2022), but less on the destruction of protocells. To understand how protocells actually emerged and evolved, it is more informative to investigate the conditions *destructive* to protocells than the conditions *conducive* to their formation. This is because destruction ultimately shapes what persists, similar to the concept of natural selection (section 2.3), where what is not selected out is what can then be passed forwards. Applying this to protocells, the geochemical conditions that cause their destruction, such as divalent cations causing aggregation, can explain how selective factors shaped the chemical characteristics cellular life took. Selection provides a powerful explanation for how certain features emerged in cellular life, and in this research the conditions that lead to aggregation resistance in protocells indicate what features early life developed in adaptation to cations in solution. This is the conceptual basis for the choice of aggregation as a measure for the effects of iron and other chemical conditions on shaping protocell evolution.

4. Methods

The experiments conducted for this project were focused on measuring the aggregation of lipid vesicles in the presence of Fe^{2+} and other cations to explore the relative effect of cations on vesicle stability and protocell assembly. A full protocol for the experimental methods and material list can be found in Appendix 1. Aggregation was observed to cause a visible increase in turbidity of the

solution (Figure 7) and spectrophotometry (400 nm) was utilized to measure the increase in light absorbance with increasing aggregation and turbidity upon addition of cations to solution.

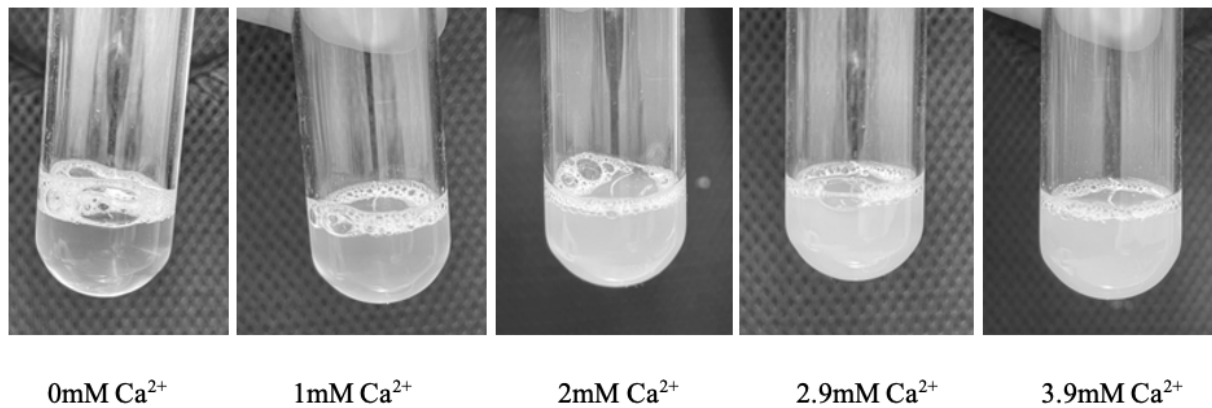


Figure 7: Fatty acid vesicle solution (LAGML, 10 mM, pH7.5) increasing in turbidity with addition of Ca²⁺ (CaCl₂, 100 mM) in 20 μ L increments.

To validate that increased turbidity such as that shown in Figure 7 is caused by the physical effect of cations interacting with lipid vesicles, micrographs (Figure 8) were taken to provide a visual demonstration of the result of aggregation and vesicle instability caused by divalent cations both with and without RNA encapsulated.

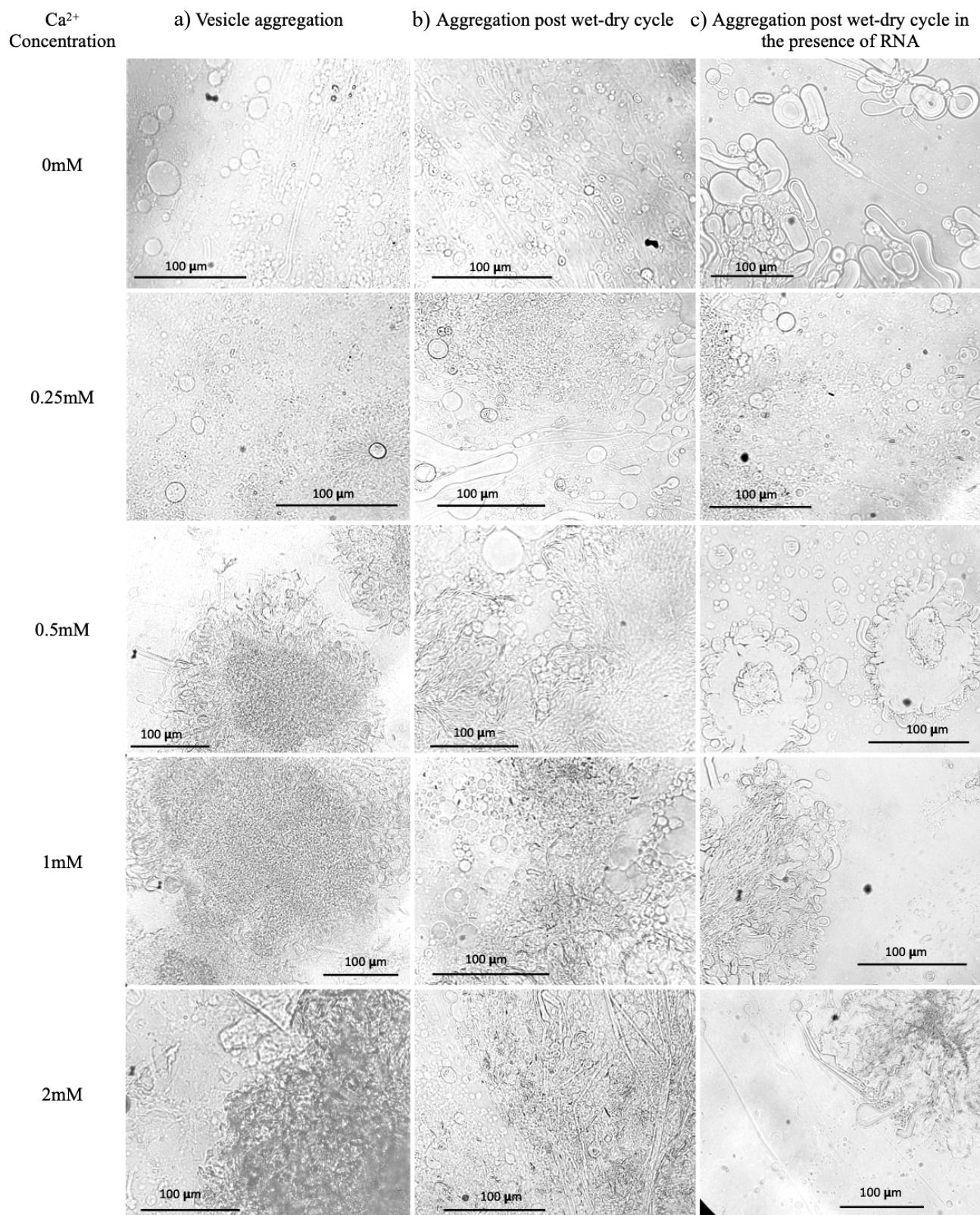


Figure 8: Micrographs of lipid vesicles aggregating in the presence of Ca²⁺. Column a) shows LAGML (100 mM) solutions increasing in aggregation with increasing Ca²⁺ exposure. Column b) similarly shows

aggregation of LAGML vesicles (100 mM), but following one wet-dry cycle, which reduced aggregation compared to column a). Column c) also shows LAGML vesicle solutions (50 mM) aggregating following a wet-dry cycle, but with RNA (2:1) included in the solution, the vesicles are stabilized in the presence of Ca^{2+} and less aggregation occurs compared with columns a) and b). Ca^{2+} cations were supplied by CaCl_2 (1000 mM) and LAGML solutions containing 0-2 mM CaCl_2 were observed via microscopy in plain optical light at 40X magnification.

Ca^{2+} cations were chosen for this demonstration as they are not as sensitive to the oxidizing atmosphere as Fe^{2+} . Anaerobic microscopy was not feasible, so experiments with Ca^{2+} could be visually examined under a microscope, whereas experiments with Fe^{2+} could not. Lipid vesicles were made of lauric acid ('LA') and glycerol monolaurate ('GML') in a 1:1 by weight ratio to make 'LAGML' vesicles (100 mM), and were prepared in TEA buffer (10 mM, pH 7.5) by warming to ~40 °C and vortexing for 30 seconds. Ca^{2+} was supplied in the form of CaCl_2 (100 mM stock solution), and was titrated into LAGML samples in increments of 5 μL , for final concentrations of 0, 0.2, 0.5, 1, and 2 mM CaCl_2 , sequentially. Samples were observed using plain light microscopy (40X magnification), and a micrograph was taken after each 5 μL addition of cation solution. The effect of cations was observed on three types of samples: plain LAGML without a 'wet-dry' cycle (Figure 8a), LAGML after one wet-dry cycle (Figure 8b), and LAGML after one wet-dry cycle in the presence of RNA (Figure 8c). Samples undergoing wet-dry cycling with and without RNA were allowed to evaporate on the microscope slide on a hot plate, then were 'rehydrated' with TEA buffer (one wet-dry cycle). The concentration of LAGML was 100 mM in the final sample without RNA, and 50 mM in samples with RNA due to practical difficulties associated with dissolving RNA at high concentrations.

4.1. Aggregation of lipid vesicles in the presence of cations

Lipid vesicles solutions were prepared as outlined in Table 1, with various mixtures of lauric acid, capric acid, and glycerol monolaurate for aggregation experiments to investigate the effect of cations on vesicle stability.

Table 1: Vesicle preparation reference key, where lipids were prepared for aggregation experiments to make vesicles composed of various mixtures of lauric acid (LA), capric acid (CA), glycerol monolaurate (GML), and RNA in buffer.

‘LAGML’	‘CAGML’	‘LAGML (acidic)’	‘LA’	‘LACA’	‘RNA-LAGML’
Lauric acid (LA, 12 carbons) and glycerol monolaurate (GML) (1:1 by weight) in 10 mM TEA pH 7.5	Capric acid (CA, 10 carbons) and glycerol monolaurate (GML) (1:1 by weight) in 10 mM TEA pH 7.5	LAGML in 10 mM MES pH 5.5	Pure LA in 10 mM TEA pH 7.5	LA and CA (1:1 by weight) in 10 mM TEA pH 7.5	LAGML and yeast RNA in a 4:1 ratio in 10 mM TEA pH 7.5, subjected to 1 wet-dry cycle

Cation solutions were prepared (100 mM), warmed (to ~40 °C) in a hot bath along with the vesicle solutions. Then 2 mL of the vesicle solution was pipetted into a 1 cm² disposable plastic cuvette, and the cation solution was titrated into the cuvette in small volumes (5-10 µL at a time) and mixed by pipetting up and down. The solution was analyzed via spectrophotometry (400 nm) ~2 minutes after cation addition. For each sample, aggregation was observed by measuring the light absorbance of turbid solutions using a spectrophotometer. Turbidity results in a reduction of the light that can pass through the solution (absorbance) and an increase in light scattering. The physical effect caused by aggregation was verified with microscopy (Figure 8).

Fe²⁺ samples were prepared with ferrous sulfate (FeSO₄), Ca²⁺ with calcium chloride (CaCl₂), and Mg²⁺ with magnesium sulfate (MgSO₄), except for the preliminary experiment in section 5.2 which used ferrous ammonium sulfate (Fe(NH₄)₂(SO₄)₂) for Fe²⁺ samples and ferric ammonium sulfate (FeNH₄(SO₄)₂) for Fe³⁺ samples to control the oxidation state of iron for direct comparison of the impact on aggregation.

4.2. Aggregation of lipid vesicles with encapsulated RNA in the presence of cations

An RNA-LAGML vesicle solution was prepared by weighing 0.06 g LAGML and 0.015 g RNA (4:1 ratio) in 5 mL TEA buffer pH7.5 (50 mM LAGML) (see Table 1, section 4.1). The solution was warmed to ~40 °C, vortexed for one minute, and heated on a hot plate until all the liquid had evaporated. 25 mL of TEA buffer was added to the dehydrated film immediately prior to the experiment (creating a final concentration of 10 mM LAGML), and the solution was warmed again and mixed by pipetting up and down. 100 mM cation solutions (FeSO₄, CaCl₂, MgSO₄) were prepared and titrated into the RNA-LAGML solution, and the resulting samples were analyzed by spectrophotometry (400 nm) as in section 4.1 and outlined in Appendix 1.

Prior to experimentation, to verify that lipid vesicles can encapsulate RNA in a 4:1 ratio following one wet-dry cycle, acridine orange dye was included in the rehydration step to stain the RNA and the sample was observed under the microscope. Acridine orange is visible in plain light when concentrated inside a lipid vesicle (Figure 9). An RNA-LAGML sample including acridine orange was prepared by pipetting 40 µL of the 50 mM RNA-LAGML solution onto a glass slide, which was allowed to evaporate on a hot plate, then rehydrated with 20 µL of TEA buffer (10 mM) and acridine orange (1 mM) solution, to make a final concentration of 100 mM LAGML on the

slide (Figure 9). Note that this was a higher concentration than analyzed via spectrophotometry, to observe the features easily and comparably to Figure 8 under the microscope.

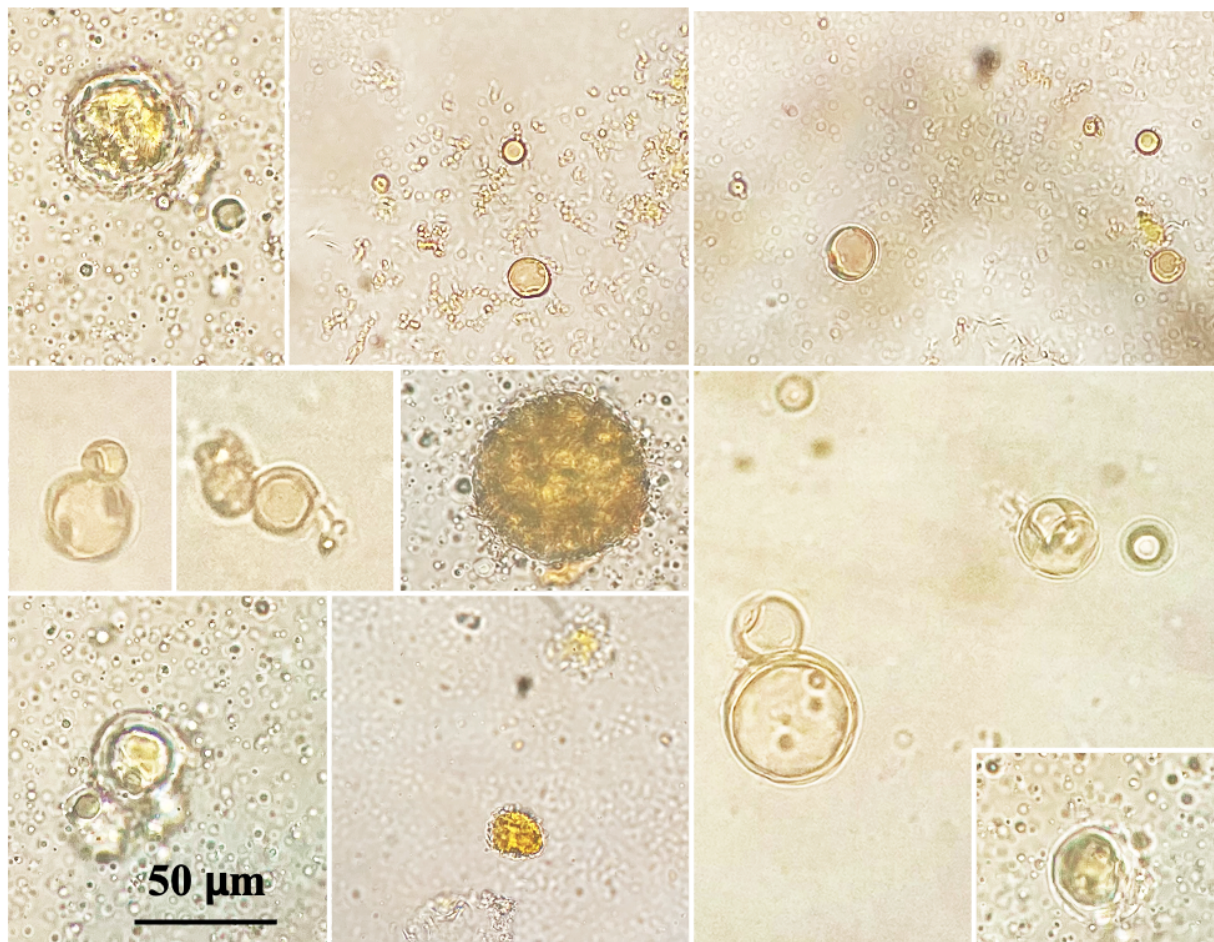


Figure 9: RNA stained with acridine orange concentrated inside LAGML vesicles, following one wet-dry cycle (encapsulation), in plain light microscopy at 40X magnification.

4.3 Note on uncertainty, replicates, and natural variability of data

For the results that follow (Figures 10-15), uncertainty margins encompass the range of measurements between replicate data, and were calculated as the standard deviation for each data point (they are not standard error). Each experiment was performed three times to create true replicates, rather than replicate analysis, to calculate the standard deviation and encompass the

natural variability between replicate samples. Aggregation is a physical phenomenon that produces heterogeneous samples, so the uncertainty margins can be large and overlap between experiments. The conclusions drawn from the experiments are derived from the averaged data, which does not overlap, and shows a consistent trend in the data across all experiments (summarized in section 5.5), indicating a robust and reproducible relationship.

Standard deviation is calculated as:

$$s = \sqrt{\frac{1}{(n-1)} \sum_{i=1}^n (x_i - \bar{x})^2},$$

s = standard deviation of a sample, n is the sample size, x_i are the individual sample values, and \bar{x} is the sample mean.

5. Results

5.1 Microscopy

Aggregation of lipid vesicles in the presence of cations is observed in section 4.1, Figure 8. At 0.5 mM, Ca^{2+} in samples of LAGML vesicles begin to form large aggregates that are visible on the micro- and macroscale ($\sim 200 \mu\text{m}$ in diameter in Figure 8a). Aggregation optically reduces the amount of light passing through the solution, observed in Figure 8 where aggregates appear as dark gray spots under the microscope and thus are scattering more light.

Among columns a) b) and c) in Figure 8 there is also a noticeable difference in the morphology of the vesicles themselves, in that there are more vesicles with multiple layers of membranes, aka ‘multilamellar’ vesicle structures, in columns b) and c). After one wet-dry cycle, multilamellar structures appear (Figure 8b), and after one wet-dry cycle in the presence of RNA, most of the vesicles appear to be multilamellar (Figure 8c).

Figure 8 also demonstrates that wet-dry cycling influences vesicle formation, particularly in the presence of RNA. After even just one wet-dry cycle, at concentrations of Ca^{2+} that usually cause mass aggregation and destabilize lone vesicles (2 mM), vesicles are still able to form in the original solution despite aggregation also occurring. In the presence of RNA, this effect is even more noticeable, indicating that RNA stabilizes membrane vesicles in the presence of calcium cations.

5.2 Iron oxidation state in solution

Fe^{2+} solutions under anaerobic conditions showed evidence of oxidation immediately after preparation and formed noticeable precipitates in buffer solutions. However, in one early experiment using ferrous ammonium sulfate, Fe^{2+} did not immediately oxidize, but remained reduced throughout the experiment. In this experiment the Fe^{2+} from ferrous ammonium sulfate caused a comparable amount of aggregation of LAGML (lauric acid & glycerol monolaurate) vesicles to Fe^{3+} cation solutions derived from ferric ammonium sulfate (Figure 10), indicating that the oxidation state of iron has only a small impact on aggregation. The effect of NH_4^+ cations from ammonium sulfate on LAGML solutions and possible interference with Fe^{2+} and Fe^{3+} results was also investigated and found to cause an increase in absorbance but not to readily induce formation of aggregates.

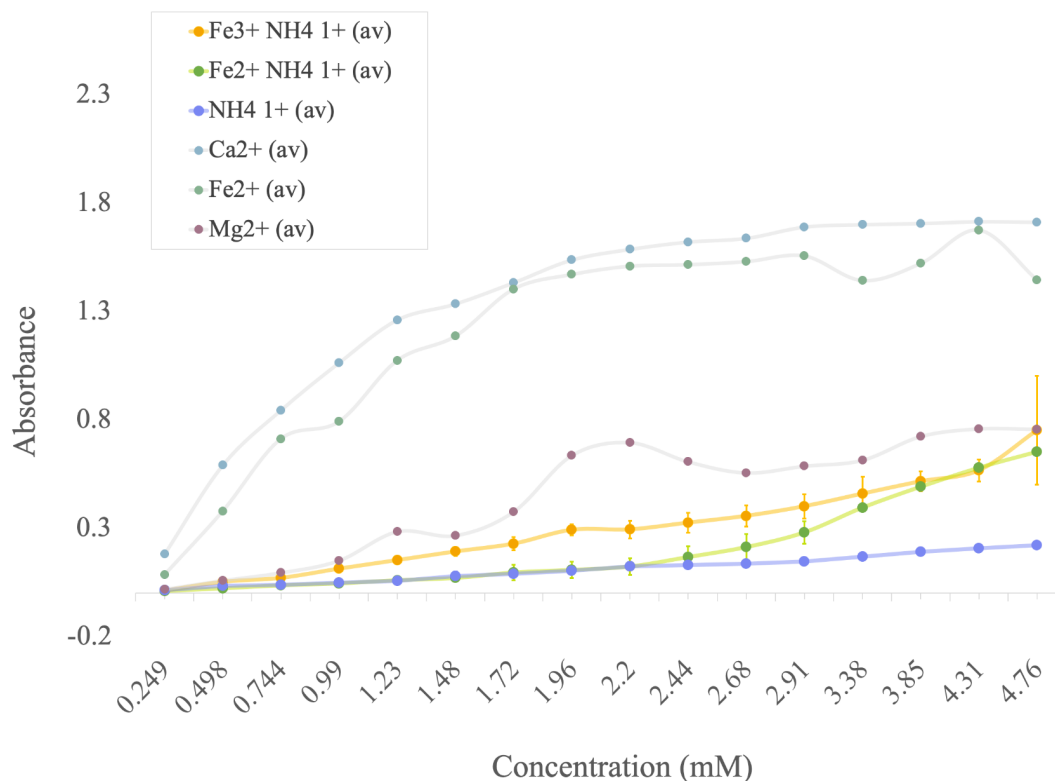


Figure 10: Light absorbance of LAGML lipid vesicle solutions with increasing concentrations of ferrous and ferric iron. High absorbance readings reflect high amounts of aggregation and unfavorable conditions for protocell formation. Samples were analyzed using spectrophotometry at 400 nm under anaerobic conditions. LAGML solutions were 10 mM in concentration, and cation concentrations between 0-4.76 mM of ferrous iron ($\text{Fe}(\text{NH}_4)_2(\text{SO}_4)_2 \cdot 6\text{H}_2\text{O}$) and ferric iron ($\text{Fe}(\text{NH}_4)(\text{SO}_4)_2 \cdot 12\text{H}_2\text{O}$) were analyzed. Ammonium sulfate ($(\text{NH}_4)_2\text{SO}_4$) included as a constant. Uncertainty margins calculated as the standard deviation for $n=3$ replicates.

5.3 Lipid vesicle aggregation with calcium, iron, and magnesium

Light absorbance was revealed to be a useful tool for discerning the effect of cations and environmental variables on lipid vesicle aggregation. Across all experiments (Figures 8–15), an increase in lipid vesicle aggregation corresponded with an increase in absorbance (y axis) caused by calcium, iron, and magnesium was discernible for each cation across variable pH conditions, vesicle compositions, and RNA wet-dry cycling. As outlined in section 2.4, cation-induced aggregation prevents fatty acids from forming vesicles and destabilizes vesicles in solution.

Therefore, a lower absorbance reading in the following results corresponds to lower amounts of aggregation and is evidence for greater vesicle survivability, and, a high absorbance reading reflects high amounts of aggregation and unfavorable conditions for protocell formation.

Across all samples, there was a clear relationship between the amount of aggregation triggered by the presence of calcium, iron, and magnesium. Calcium (blue) produced the most aggregation, followed closely by iron (green), whereas magnesium (pink) produced the least aggregation (Figure 11). This relationship is abbreviated by ‘ $\text{Ca}^{2+} > \text{Fe}^{2+} > \text{Mg}^{2+}$ ’ in the following results.

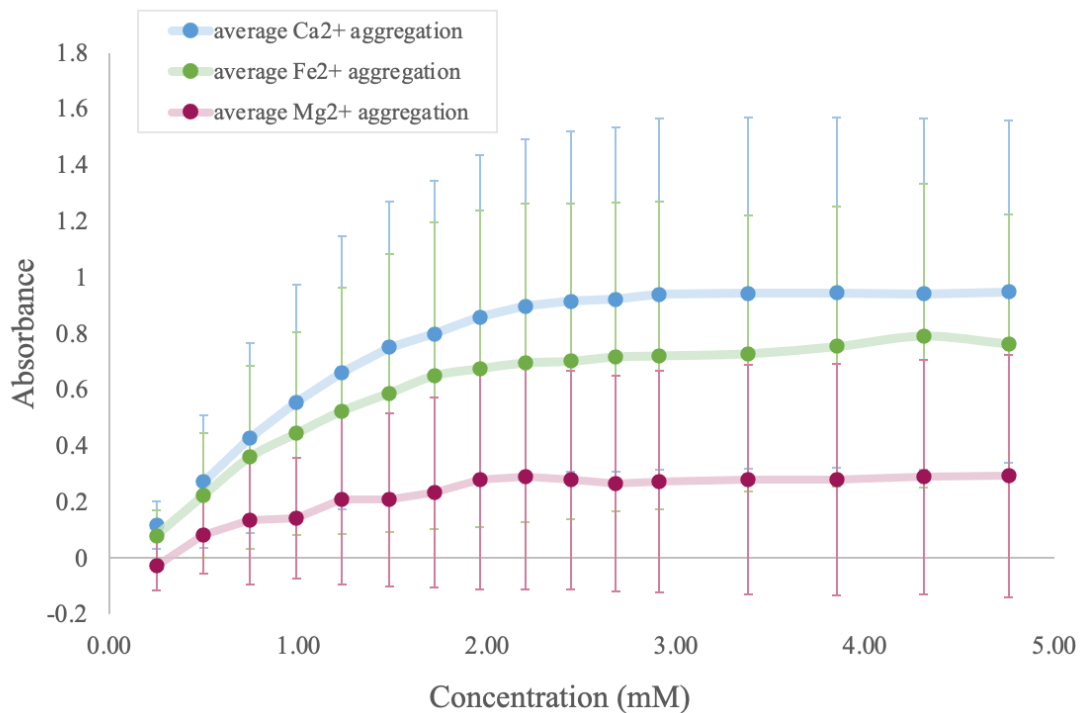


Figure 11: Increasing absorbance (aggregation) with increasing concentration of calcium, iron, and magnesium cations. The average aggregation for each cation is plotted as solid lines, with uncertainty bars representing the standard deviation for each cation accounting for all experiments (LAGML, LAGML pH 5.5, CAGML, LA, LACA, RNA-LAGML). High absorbance readings reflect high amounts of aggregation and unfavorable conditions for protocell formation. Calcium (blue) produces the most aggregation, followed closely by iron (green), and magnesium (pink). Uncertainty margins calculated as the standard deviation for n=3 replicates.

5.3.1 Lipid vesicles in neutral and acidic pH

Under acidic conditions (pH 5.5), absorbance readings and aggregation of LAGML vesicles (made of lauric acid & glycerol monolaurate) were lower than in neutral conditions (pH 7.5), as seen in Figure 12. Both pH conditions showed evidence of LAGML aggregation in the presence of Ca^{2+} , Fe^{2+} and Mg^{2+} , where the relative effect of each is consistent with the Ca^{2+} (1) Fe^{2+} (2) Mg^{2+} (3) relationship seen in Figure 11.

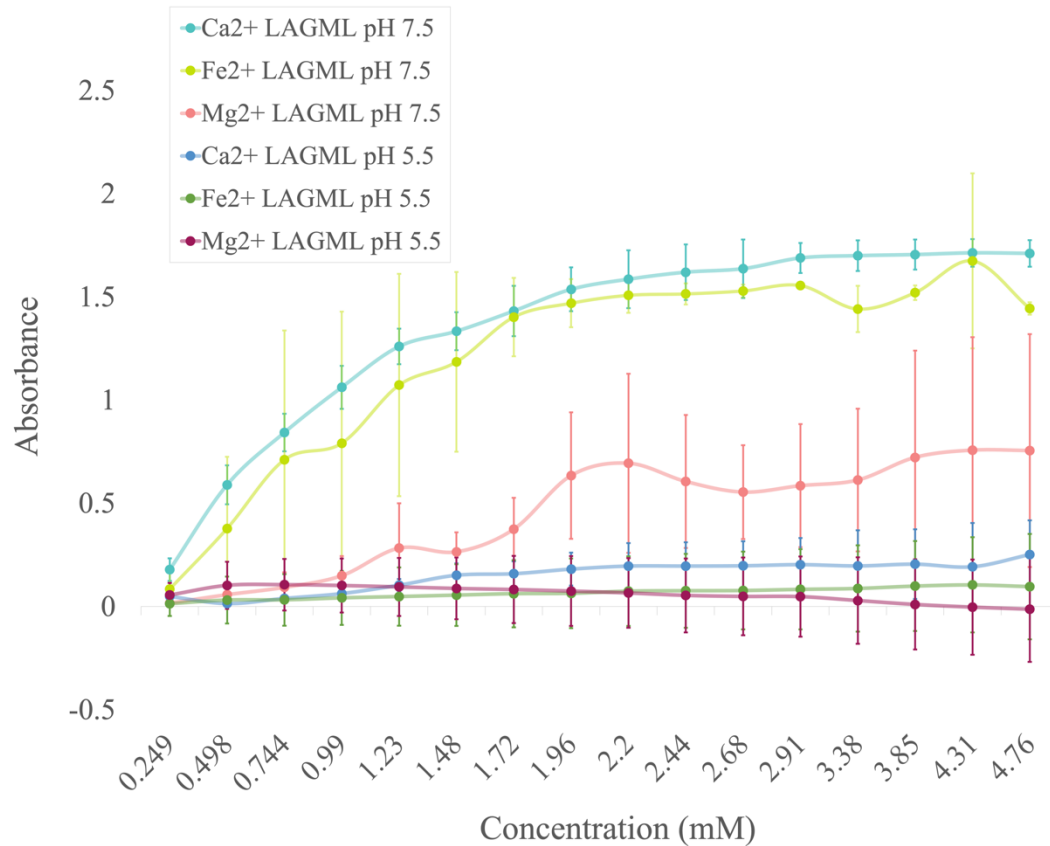


Figure 12: Light absorbance of LAGML lipid vesicle solutions with increasing cation concentrations, pH 7.5 and pH 5.5. High absorbance readings reflect high amounts of aggregation and unfavorable conditions for protocell formation. Samples were analyzed using spectrophotometry at 400 nm under anaerobic conditions. LAGML solutions were 10 mM in concentration, and cation concentrations between 0-4.76 mM. Fe^{2+} samples were prepared with ferrous sulfate (FeSO_4), Ca^{2+} with calcium chloride (CaCl_2), and Mg^{2+} with magnesium sulfate (MgSO_4). Uncertainty margins calculated as the standard deviation for $n=3$ replicates.

5.3.2 Lipid vesicles made of LAGML and CAGML

Vesicles made of CAGML (capric acid & glycerol monolaurate), had lower absorbance readings than vesicles that were made of LAGML (Figure 13). Vesicles made of CAGML increased in turbidity in the presence of Ca^{2+} , Fe^{2+} and Mg^{2+} cations, with their relative effect on aggregation being Ca^{2+} (1) Fe^{2+} (2) Mg^{2+} (3). However, Fe^{2+} surpassed the absorbance and aggregation produced by Ca^{2+} at concentrations of ~ 2.91 mM, beyond which absorbance and aggregation continued to increase.

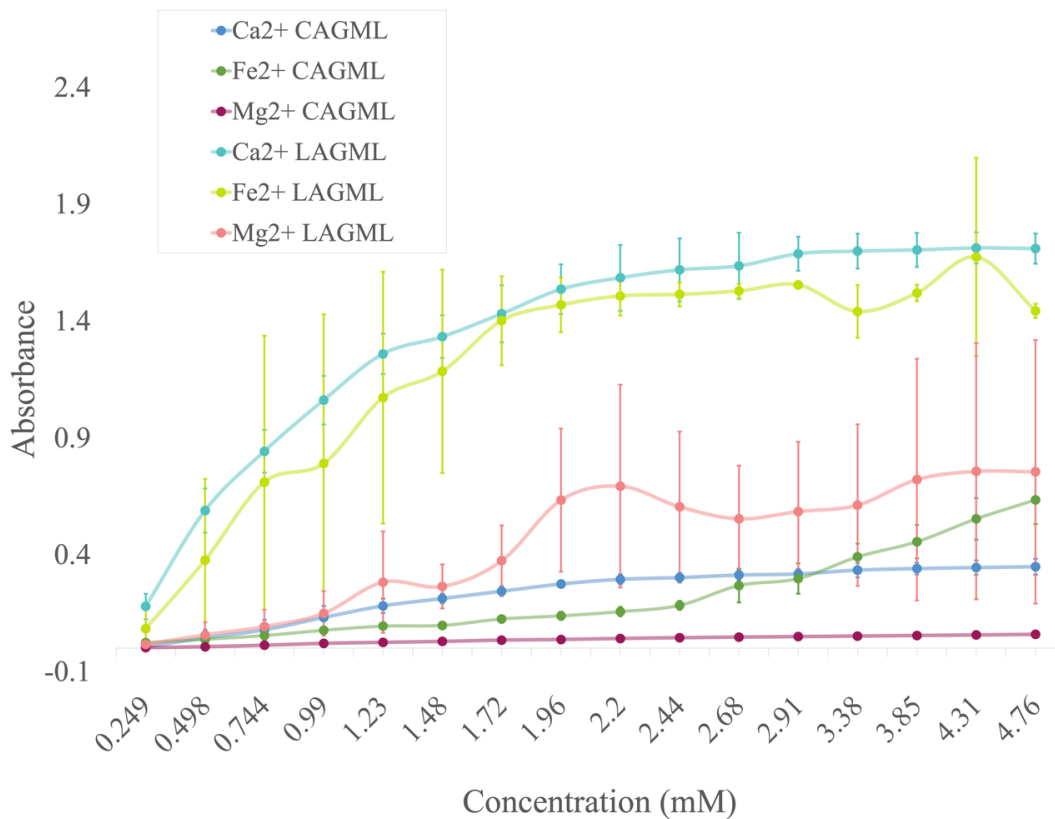


Figure 13: Light absorbance of LAGML and CAGML lipid vesicle solutions with increasing cation concentrations, pH 7.5. High absorbance readings reflect high amounts of aggregation and unfavorable conditions for protocell formation. Samples were analyzed using spectrophotometry at 400 nm under anaerobic conditions. LAGML and CAGML solutions were 10 mM in concentration, and cation concentrations between 0-4.76 mM. Fe^{2+} samples were prepared with ferrous sulfate (FeSO_4), Ca^{2+} with calcium chloride (CaCl_2), and Mg^{2+} with magnesium sulfate (MgSO_4). Uncertainty margins calculated as the standard deviation for $n=3$ replicates.

5.3.3 Lipid vesicles made of LA and LACA

Vesicles made of LA (lauric acid), had lower absorbance readings (i.e., less aggregation) than vesicles that were made of LACA (lauric acid and capric acid) (Figure 14). Vesicles made of both LA and LACA showed evidence of aggregation in the presence of Ca^{2+} , Fe^{2+} and Mg^{2+} cations (Ca^{2+} (1) Fe^{2+} (2) Mg^{2+} (3) relative aggregation).

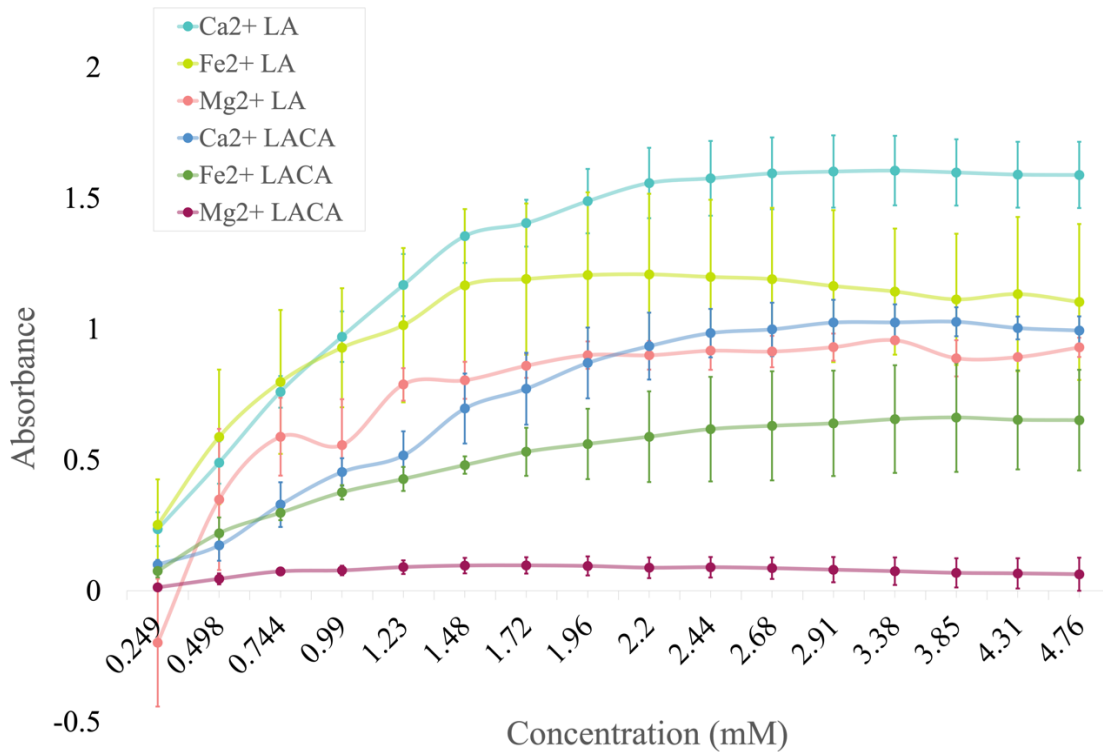


Figure 14: Light absorbance of LA and LACA lipid vesicle solutions with increasing cation concentrations, pH 7.5. High absorbance readings reflect high amounts of aggregation and unfavorable conditions for protocell formation. Samples were analyzed using spectrophotometry at 400 nm under anaerobic conditions. LA and LACA solutions were 10 mM in concentration, and cation concentrations between 0-4.76 mM. Fe^{2+} samples were prepared with ferrous sulfate (FeSO_4), Ca^{2+} with calcium chloride (CaCl_2), and Mg^{2+} with magnesium sulfate (MgSO_4). Uncertainty margins calculated as the standard deviation for $n=3$ replicates.

5.3.4 Lipid vesicles made of LAGML and RNA

LAGML vesicle samples (composed of lauric acid & glycerol monolaurate) that underwent one wet-dry cycle in the presence of RNA had lower absorbance readings (i.e., less aggregation) than LAGML samples that did not contain RNA (Figure 15). RNA-LAGML samples still increased in turbidity in the presence of Ca^{2+} , Fe^{2+} and Mg^{2+} cations, with their relative effect on aggregation being Ca^{2+} (1) Fe^{2+} (2) Mg^{2+} (3).

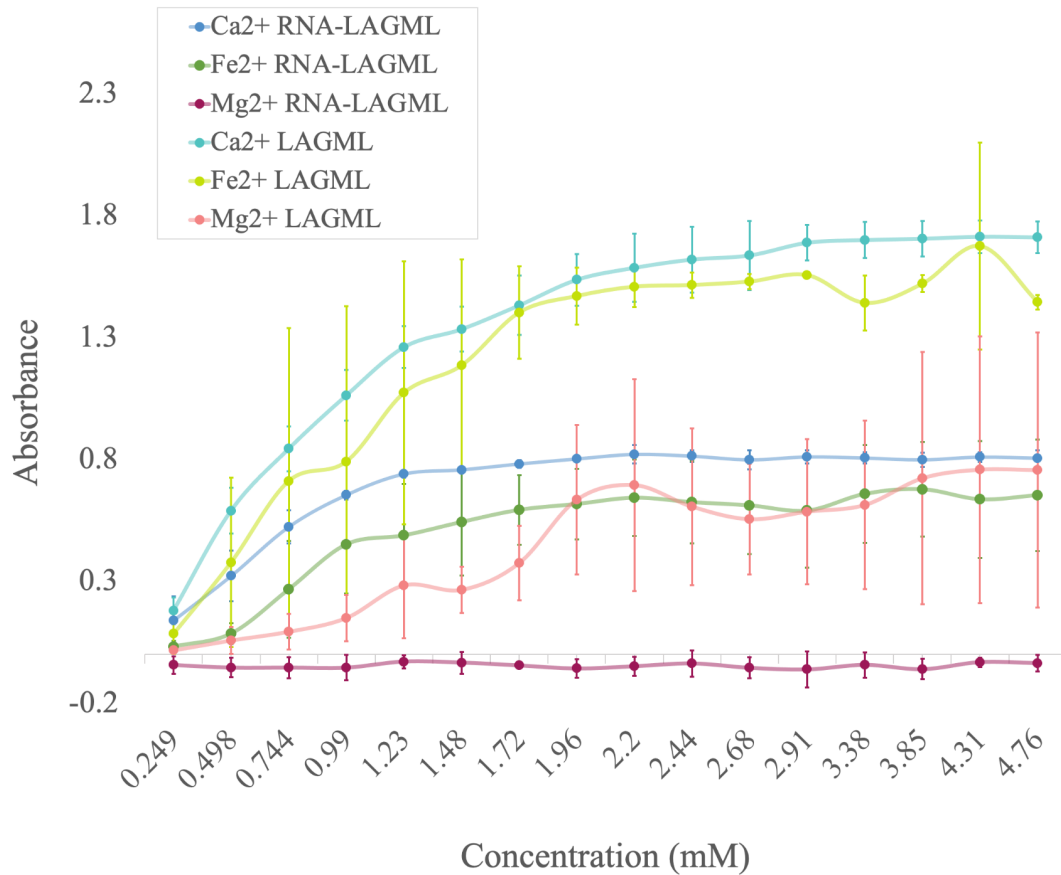


Figure 15: Light absorbance of LAGML and RNA-LAGML lipid vesicle solutions with increasing cation concentrations, pH 7.5. High absorbance readings reflect high amounts of aggregation and unfavorable conditions for protocell formation. Samples were analyzed using spectrophotometry at 400 nm under anaerobic conditions. LAGML was 10 mM in solution in a 4:1 ratio with RNA, and cation concentrations of 0-4.76 mM. Fe^{2+} samples were prepared with ferrous sulfate (FeSO_4), Ca^{2+} with calcium chloride (CaCl_2), and Mg^{2+} with magnesium sulfate (MgSO_4). Uncertainty margins calculated as the standard deviation for $n=3$ replicates.

5.4 Temperature and aggregation (preliminary observations)

The highest absorbance readings (seen with LAGML and LA samples) were recorded for the lower range of temperatures used in the experiments. However, at lower temperatures there were also some low absorbance readings (LAGML pH 5.5 samples). Samples with low absorbance readings, RNA-LAGML, LACA, CAGML, and LAGML pH 5.5, showed less variability in absorbance over a range of temperatures. Vesicles analyzed well below the ‘phase transition’ of the fatty acids have higher absorbances at lower temperatures. No direct experiment testing the same sample’s absorbance over the full range of temperatures was conducted.

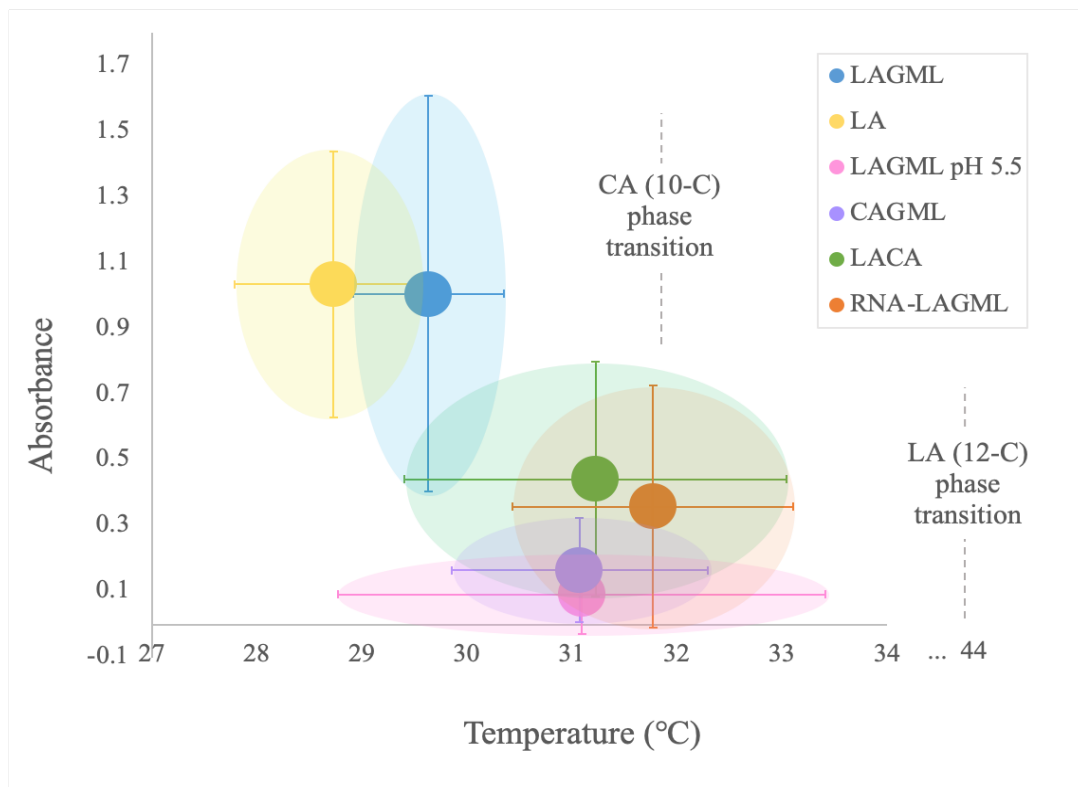


Figure 16: Average light absorbance of 10 mM lipid vesicle solutions (LAGML, LAGML pH 5.5, CAGML, LA, LACA, RNA-LAGML) vs. temperature (Celsius). Standard deviations show as bars and bubbles.

5.5 Summary of results

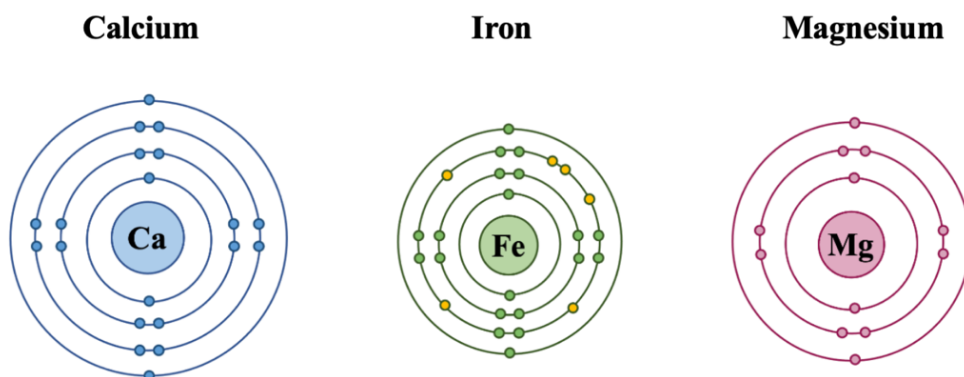
- Lipid vesicles across all experiments (Figures 10-14) showed different sensitivities to Ca^{2+} , Mg^{2+} , and Fe^{2+} . There is clear pattern of Ca^{2+} causing the most aggregation, followed closely by Fe^{2+} , with the least aggregation caused by Mg^{2+} cations.
- LAGML solutions (pH 7.5) showed the greatest tendency for aggregation compared to other vesicle solutions.
- Vesicle solutions in acidic pH conditions, or those containing CA or RNA, had lower absorbance readings (i.e., less aggregation) than those under neutral pH conditions and those made with LA.
- There is preliminary evidence for absorbance (and hence aggregation) being impacted by temperature.

6. Discussion

6.1 Role of atomic properties on cation-induced vesicle aggregation

As outlined in section 5.5, although the cations tested all have the same ionic charge (+2), they elicit different effects on fatty acid aggregation. Differences in valence electrons in the outer electron shell of atoms typically have the greatest impact on the behavior of the cation. However, given that calcium, iron and magnesium cations all have a filled outer shell of valence electrons (2+ charge), variation in cation behavior with fatty acids in solution must be explained by a combination of other factors at the atomic scale. We consider four such factors: 1) capacity to interact strongly with anions; 2) how highly hydrated the cation is; 3) atomic radii; and 4) solubility in water (Table 2).

Table 2: Summary of the atomic properties of calcium, iron, and magnesium that affect interactions with fatty acids and water.



factor	atomic property	Calcium	Iron	Magnesium
1	d-orbital (●) configuration	empty (0)	half (6)	empty (0)
	Type of interaction	electrostatic	covalent	electrostatic
	Bond length	long	short	short
2	Preferred hydration shell	6-12 bound water molecules	4-6 bound water molecules	6-8 bound water molecules
3	Atomic radius (nm)	0.197	0.126	0.16
4	Solubility	low	intermediate	high

In order to compare how calcium, iron and magnesium cations interact with water and carboxylate groups, it is necessary to understand the electron configuration of each, which determines the type of interaction as well as the how specific the orientation of the interaction is. Calcium and magnesium have no ‘d-orbitals’ in their electron shell configuration, since the principal quantum numbers of the divalent cations ($n = 2$ and $n = 1$, respectively) allow for only s and p orbitals. This reduces the ability of calcium and magnesium cations to form strong bonds with other species and they therefore interact through charge-dipole electrostatic attractions rather than covalently. Ferrous iron, however, has six electrons in its d-subshell orbital, leaving empty d

orbitals that can participate in covalent interactions. Note that the interactions possible with the d-orbital electron arrangement of iron have a highly specific number and orientation, typically interacting with six molecules in an octahedral geometry, whereas for calcium and magnesium, electrostatic interactions allow binding in many different directions.

The interaction each cation has with water is related to the type of bonding described above, wherein iron forms covalent coordination bonds to water, and calcium and magnesium bond to water through weaker charge-dipole interactions. The amount of water each cation interacts with (and the strength of this interaction) is also affected by atomic radius. Hydration of atoms increases with atomic charge and has an inverse relationship with cation size. The more electron shells and larger the atomic radii, the more the nuclear charge is concealed from other molecules, leading to weaker interactions with water. Even though calcium has the largest atomic radius (relative to iron and magnesium) and can hold the most water molecules around it (up to 12 or so), the length of the bond between calcium ions and water molecules is greater than that between iron or magnesium and water. This makes the strength of the binding of Ca^{2+} to water weaker, resulting in low solubility in water. Magnesium has a smaller atomic radius than calcium but is a much more strongly hydrated ion. This is because magnesium can hold the water molecules closer to its nucleus because of the shortened bond length and smaller atomic radius, despite being capable of holding fewer water molecules than calcium (6-8). Iron binds to water (and other molecules) covalently, so has shorter bond lengths to water molecules than calcium, similar to magnesium. Iron also is only able to hold four to six water molecules, but despite this, the strength of the bond exceeds those of both calcium and magnesium because of the covalent nature of the bonding (highly specific, but strong), and thus iron can be easily hydrated. For example, Fe^{2+} is more soluble than Fe^{3+} , because Fe^{3+} is more stable in iron-oxide solid form than in solution.

Additionally, Fe^{3+} solubility is sensitive to pH in comparison to Fe^{2+} , as Fe^{3+} is relatively insoluble unless the conditions are acidic. Given that the solubility of iron is dependent largely on oxidation state and pH (section 3.2.1), iron's solubility has been simplified as 'intermediate' in Table 2.

In summary, the role of atomic properties on fatty acid carboxylate group binding is multifactorial, and drawing conclusions based on any one factor alone leads to contradictions in theory and observation (e.g., if calcium has the lowest binding strength, why does it produce the most aggregation?). Combining an understanding of bonding strength, hydration, size, and solubility (factors 1-4, Table 2) as they differ between cations can explain the relative differences in cation-lipid aggregation reported in section 5. The broad trend of calcium, iron, and magnesium (respectively, in descending order) on relative aggregation production is consistent with their expected interactions with water and fatty acids. The atomic properties that lead to higher affinity with water (smaller size, short bond length) usually mean they have diminished interaction with carboxylate groups and contribute less to aggregation. To summarize the atomic properties of each cation as they relate to interactions with water and fatty acids:

- Calcium can bind more waters than iron or magnesium, but despite this capacity the individual interactions themselves are weaker, so calcium is less soluble in water and would preferentially bind carboxylate groups. Therefore, calcium can bind more carboxylate groups at once than iron and magnesium, resulting in greater aggregation.
- Iron binds strongly and with a highly specific orientation to both water and carboxylate groups, and this great interaction strength leads to a similar amount of aggregation to calcium, despite being able to hold less total water molecules than calcium. Iron is more soluble in water which contributes to a slight reduction in preferential interactions with carboxylate groups.

- Magnesium can hold fewer water molecules than calcium and has weaker interactions with water than does iron. However, its smaller size allows it to hold water much more closely than can calcium, which ultimately leads to a more consistently hydrated state and greater solubility in water. This means preferential binding to water over carboxylate groups, resulting in reduced contribution to aggregation.

6.1.1 Role of Mg^{2+} in protocell evolution?

Magnesium's preferential binding of water rather than fatty acid carboxylate groups could explain both why it produced less aggregation, and doesn't prevent protocell formation to the same extent as other cations do, as well as magnesium's inclusion in biological chemistry. Magnesium cations are abundant in modern prokaryotic and eukaryotic cells, with total cellular concentrations up to 25 mM and free concentrations of 0.3–1.5 mM (Dudev & Lim, 2013). This could to some degree be a product of the hydrothermal chemistry at life's origins, where highly hydrated Mg^{2+} cations were better tolerated by membrane vesicles than Ca^{2+} and Fe^{2+} . Along the evolutionary path towards modern cells, primitive membranes developed the molecular machinery to select for cations permeating through membrane pores (Deamer & Dworkin, 2005), and Mg^{2+} became useful for other cellular functions, such as polymerase ribozyme function and RNA polymerization (Schrum et al., 2010).

6.2 Environmental effects on vesicle aggregation

6.2.1 Effect of pH on vesicle formation

pH greatly affects the morphology of lipids in solution. Protonated lauric acid forms oily droplets at low pH values, micelles at high pH, and vesicles around its pKa (Deamer et al., 2019). The

interaction between carboxylate groups and metal cations is also affected by pH. Under acidic conditions, more hydronium ions are in solution, which under low enough pH (2-3) protonates carboxylate groups (given their pKa ~4) and neutralizes their anionic charge (COO⁻ → COOH), preventing metal cations from binding.

The experimental solutions examined in this work had a pH of 5.5, which would not be sufficiently acidic to protonate carboxylate groups and convert them into carboxylic acids, yet a decrease in absorbance and aggregation is observed under acidic conditions, as seen in section 5.3.1 (Figure 12). This behavior can be understood by considering the behavior of metal ions themselves. Metal cations bridge fatty acids and form coordinate bonds with multiple fatty acids at once (section 2.4), resulting in aggregation, but the strength of this interaction is pH sensitive. High pH conditions drive tight discrete coordination environments for the metal cation to the carboxylate group. At low pH, metal cations are more soluble and prefer to interact with water than carboxylate groups. This relationship is observed with other small molecules, such as peptides, which increasingly bind to metals at higher pH (Sóvágó et al., 2012), and provides an explanation of why aggregation did not readily occur at pH 5.5 (Figure 12).

The pH conditions in natural hot spring settings and between individual pools can vary greatly. For example, Whangapipiro hot spring sites in New Zealand display pH ranges from pH 1.65 to pH 8.1 within the Hells Gate hot spring (one locality at Whangapipiro) (Deamer et al., 2019). This variability encompasses the pH conditions that are conducive for lipid vesicle formation (pH near the pKa of fatty acids), aggregation and metal-polymer binding (neutral-high pH), as well as aggregation evasion (sub neutral-low pH), which overall creates a diverse landscape for selective factors essential to the evolutionary process of assembling protocells.

6.2.2 Effect of temperature on aggregation

There is some evidence that lower temperatures increase the light absorbance by, and potentially aggregation of, vesicle solutions (Figure 16). At low temperatures, larger aggregates can form, which could correspond to increased light absorbance (Figure 17, Chong & Colbow, 1976). Additionally, fatty acids gradually become insoluble as the temperature drops below their solubility temperature. As temperature increases and the solubility point of the lipid is crossed, larger multilamellar vesicles form (Chong & Colbow, 1976), and turbidity can decrease, resulting in reduced light absorbance. A combination of the increased size of aggregates and the reduced solubility of the fatty acids at low temperatures provides an explanation for the increased light absorbance seen in section 5.4 (Figure 16), but an experiment designed specifically to test the effect of increased temperatures on aggregation would be necessary to consider this further.

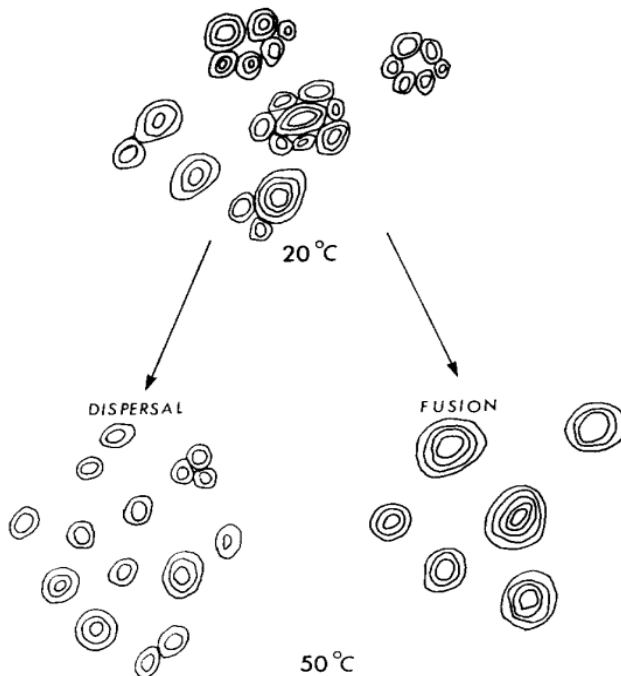


Figure 17: Physical interactions between lipid vesicles at 20 °C and 50 °C. At lower temperatures vesicles form large aggregates, and at higher temperatures aggregates disperse into individual smaller vesicles as well as fuse into larger multilamellar vesicles. Taken from Chong & Colbow (1976).

6.3 Effect of fatty acid composition

6.3.1 Effect of carbon chain length and temperature on lipid vesicle formation

Although shorter carbon chain length fatty acids are known to reduce the stability of vesicles (Deamer & Dworkin, 2005), section 5.3.2 shows evidence that they increase the stability of vesicles (decrease aggregation). This observed effect could be explained by the temperatures at which analysis took place, and the different solubilities of lauric (12 carbons) and capric acid (10 carbons). The length of the carbon chain determines the temperature at which it dissolves, and longer chain fatty acids require higher temperatures to dissolve. The solubility also reflects a phase transition in the lipid's properties, which behave as a gel and then a fluid past its 'phase transition' temperature. Capric acid's (10 carbons) phase transition temperature is ~32 °C, lauric acid's (12 carbons) phase transition temperature is ~44 °C, while palmitic acid (16 carbons) is ~64 °C (Deamer et al., 2019). The average temperature of the experiments was 30.2 °C, and although samples were maintained at >45°C in a hot bath, cooling of the sample after removal from the hot bath was inevitable and may have resulted in some fatty acids becoming insoluble (Figure 16). In the case of lauric acid, the temperature was sufficiently below the solubility limit/phase transition temperature to increase the absorbance reading as insoluble solid white aggregates appeared in solution. The implication of this is that lipid vesicles made of shorter chain length fatty acids may more readily form vesicles and resist de-solubilization at lower temperatures. The stability of different carbon chain length fatty acids is relative to the temperature and environmental conditions, and the fatty acid that forms the most stable vesicles is one whose carbon chain length is suitable to the given environmental conditions.

6.3.2 *Effect of mixed fatty acid ‘mosaic’ vesicles*

The inclusion of shorter chain fatty acids in a membrane ‘mosaic’ reduced aggregation (i.e., stabilized vesicles) as seen in section 5.3.3 (Figure 14). Mosaic vesicles were composed of a mixture of fatty acids of 12 and 10 carbon chain lengths (‘LACA’) and were analyzed at similar temperatures. The reduced amount of aggregation observed (relative to pure ‘LA’ samples) can be explained chemically by considering that pure compounds more readily form solids than mixed compounds. When the composition of fatty acids in lipid vesicles are mixed, fatty acids have better solubility and stability, and behave as a fluid mosaic in a membrane structure. Additionally, vesicles made from an array of fatty acids, 1-alkanols and isoprenoids have been shown to form stable vesicles even in seawater solutions (Jordan et al., 2019); an environment otherwise thought to be destructive to the self-assembly of vesicles (Milshteyn et al. 2018) (see Appendix 3). This mixed membrane feature is preserved in contemporary cells, where the cell membrane is composed not only of various lipids but also of other compounds such as sterols and proteins.

Scaling this relationship of mixed chemical composition and stability up to its expression in modern biology, it is helpful to consider the concept of ‘hybrid vigor’. Here the characteristics of two individuals combined to form a hybrid allows the hybridized individual to take advantage of a wider range of genetic information to respond to a larger range of environmental conditions and is therefore capable of a response that spans the diversity of the two original individuals. Lipid vesicle mosaics could be considered a prebiotic example of the same concept, whereby the combination of shorter and longer chain fatty acids inside vesicles allows stable vesicles to form over a temperature range that spans the solubility limit of both fatty acids. See schematic representation of this concept in Figure 18.

SELECTION

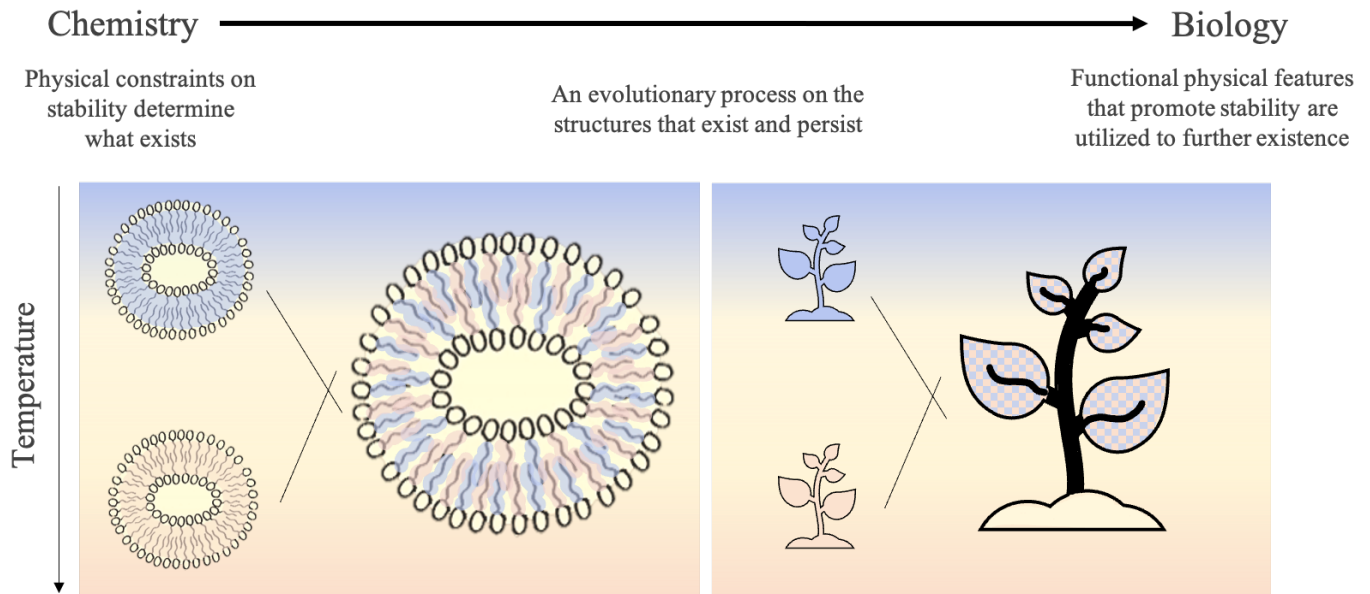


Figure 18: Modern biology contains echoes of prebiotic chemistry. 'Hybrid vigor', an example observed in biology today as potentially an echo of prebiotic chemistry, is a phenomenon where hybridized individuals are more robust than their individual predecessors, as they draw functionality from a more diverse genetic background. A schematic representation of biological hybrids above displays that hybrid plants crossbred from low and high temperature-tolerant parents to create a hybrid that is tolerant to a wider range of temperature conditions. Prebiotic hybrids in this research are mosaic fatty acid vesicles, where a mixture of short (stable at lower temperatures) and long (stable at higher temperatures) chain fatty acids increase the stability of the vesicle over a broader range of temperature conditions. Hybrid vigor could apply on the scale of molecules, retained and amplified by biology through an evolutionary process acting chemistry to life through time by a multi-scale selection process.

The observed solubility of fatty acids as they relate to aggregation in this research demonstrates a critical dependence on the experimental and natural environmental conditions. This sensitivity is important when considering origin of life environments on Earth and elsewhere, as the features we associate with early life are totally dependent on the features of the early environment in which they emerged.

6.4 Concentration of cations in natural settings

The concentration ranges of calcium, iron, and magnesium cations in natural hot spring water as collated from Deamer et al. (2019) and Wu et al. (2013) are compared to the concentrations of cations that produce aggregation in this research (Figure 19).

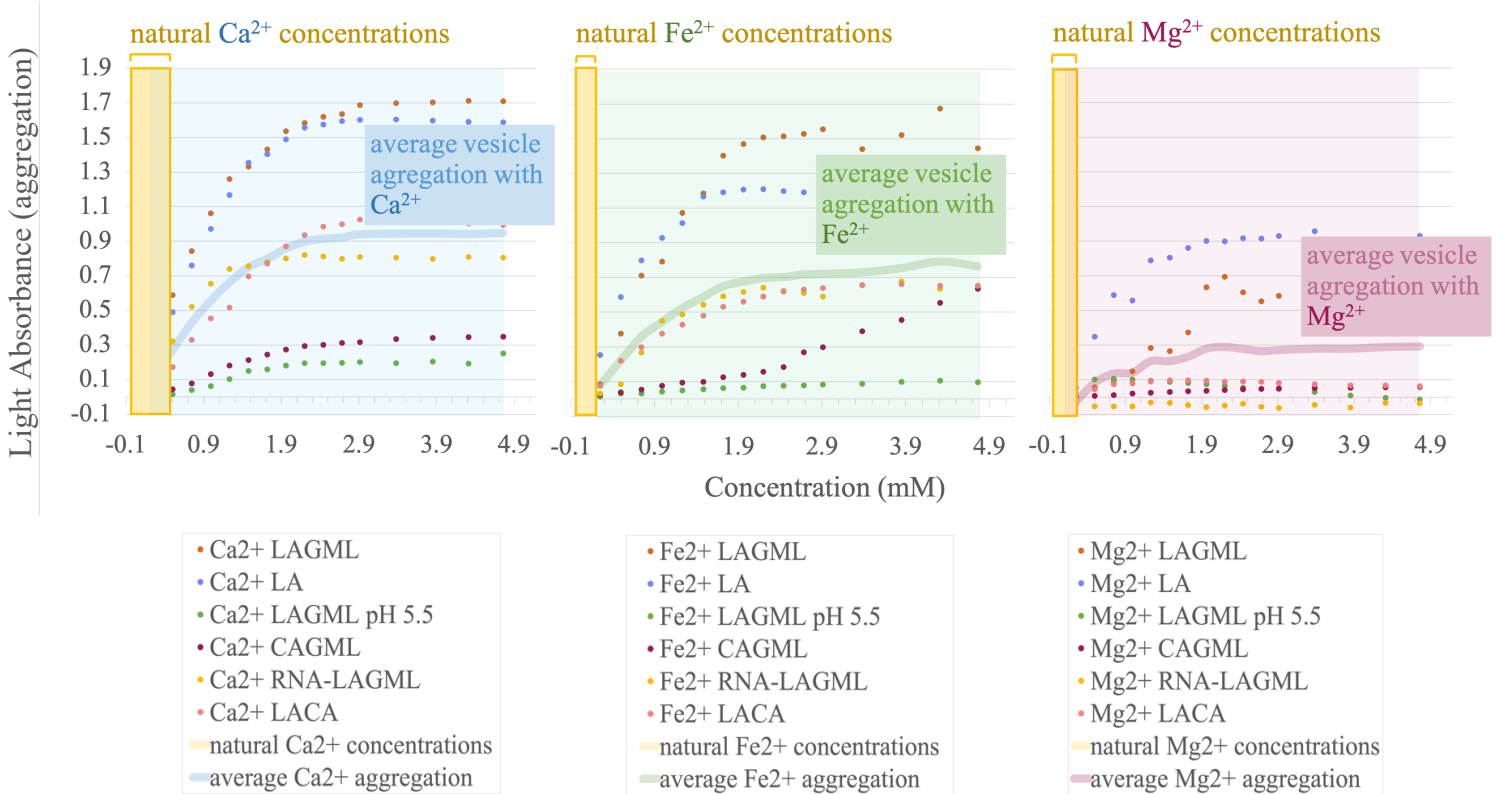


Figure 19: Cation concentrations for calcium, magnesium, and iron observed to produce aggregation in this study are much higher than the cation concentrations found in natural hot spring settings, as investigated by Deamer et al. (2019).

Hot spring sites in different countries that encompassed a variety of ionic and pH conditions were investigated by Deamer et al. (2019) and included in this comparison: Midway Geyser Basin, Norris Geyser Basin, Bison Pool, and Chocolate Pots hot springs in Yellowstone California; Hell's Gate and Whangapipiro hot springs in New Zealand; and Kamchatka hot springs in Russia. Each

site had a different relative abundance of cations in solution, for example there was highest Fe^{2+} at Chocolate Pots in Yellowstone. High iron content at Chocolate Pots and other hot springs can be due to 1) the iron-carbonate lithology (Wade et al., 1999), 2) Fe^{3+} reducing bacteria (Wu et al., 2013), and 3) acidic pH ranges (Ball et al., 2002) which keeps Fe^{2+} dissolved. Iron-carbonate lithologies are also plausible for martian hot springs (Morris et al., 2010), which we can expect to have also had a high relative abundance of iron. This means it is valuable to test the relative contributions of different cations to aggregation to understand how geochemical differences in hydrothermal systems can affect the formation of cellular life. In this research, the concentrations of cations needed to cause mass aggregation of fatty acids typically far surpass the concentrations of cations observed in these field sites. Given aggregation prevents fatty acids from forming vesicles, natural hot spring ionic conditions are far more conducive to protocell formation than the experimental conditions. However, in the case of calcium, there is a small amount of overlap between the concentrations found in the field and aggregation concentrations. Given that calcium cations produced the most aggregation in this research, the presence of Ca^{2+} in hot springs could have adversely impacted the formation of lipid vesicles.

Hot springs are affected by precipitation and evaporation cycles. This produces natural variability in the concentration of cations within the same pool over time as the water volume changes. The result could be that pools increase in cation concentration during evaporation; thus, aggregation was likely an important selective barrier for emerging protocell communities to overcome on the early Earth. Aggregation has also been observed in this research to vary with pH, temperature, and vesicle composition. This adds a combinatorial aspect to the selection occurring on vesicles in these pools, where protocells can evolve through overcoming selective barriers in the landscape based on the vesicle's physical stability in pools with different ionic compositions,

temperatures, and pH, where the survivability of a protocell community is governed by the interplay of external environmental and internal factors.

6.5 Role of RNA in protocell evolution

The co-localization of RNA precursors inside lipid vesicles is a significant step in the origin of life transition, as it allows selection processes to act on an interacting set of molecules, rather than on individual molecules alone. The combination of RNA inside a vesicle can be thought of as an ‘emergent’ structure in chemistry, where the combined function of RNA and lipids together create a larger ‘whole’ which acts as a new subject of evolution. As seen in section 5.1 (Figure 8) and 5.3.4 (Figure 15), there is a significant impact on lipid vesicle morphology and an increase in stability when vesicles self-assemble in the presence of RNA. The factors contributing to this result are described below, along with speculation on the physical and chemical effect of RNA-lipid interactions under wet-dry cycling conditions.

6.5.1 RNA-fatty acid interaction during wet-dry cycling

When lipid solutions are heated, water evaporates while lipids and other dissolved contents dry down into a concentrated film (Figure 20). This evaporative process allows progressive molecular crowding to take place, and any lipid vesicles in the solution can fuse their membranes and create parallel layers of lipids that can serve as ‘highways’ for molecular polymer transport in the intermediate phase between wet and dry (Damer & Deamer, 2020). Given that RNA monomers can bind to fatty acid vesicles made of capric acid (Black et al., 2013), it is possible that the wet-dry cycling allows for RNA to come into close contact with the lipids, which may allow for binding to occur. This interaction could be preserved in the wet phase whereby RNA is bound to self-assembled membranes and is observed to stabilize them in the face of cations in solution. This

conjecture is supported by Figure 13 (section 4.2), which demonstrates that RNA stained by acridine orange is more concentrated inside the vesicles than in the free solution following one wet-dry cycle, but further investigation is needed to determine exactly where the RNA is located inside the protocells to understand whether binding has occurred during the wet-dry cycle.

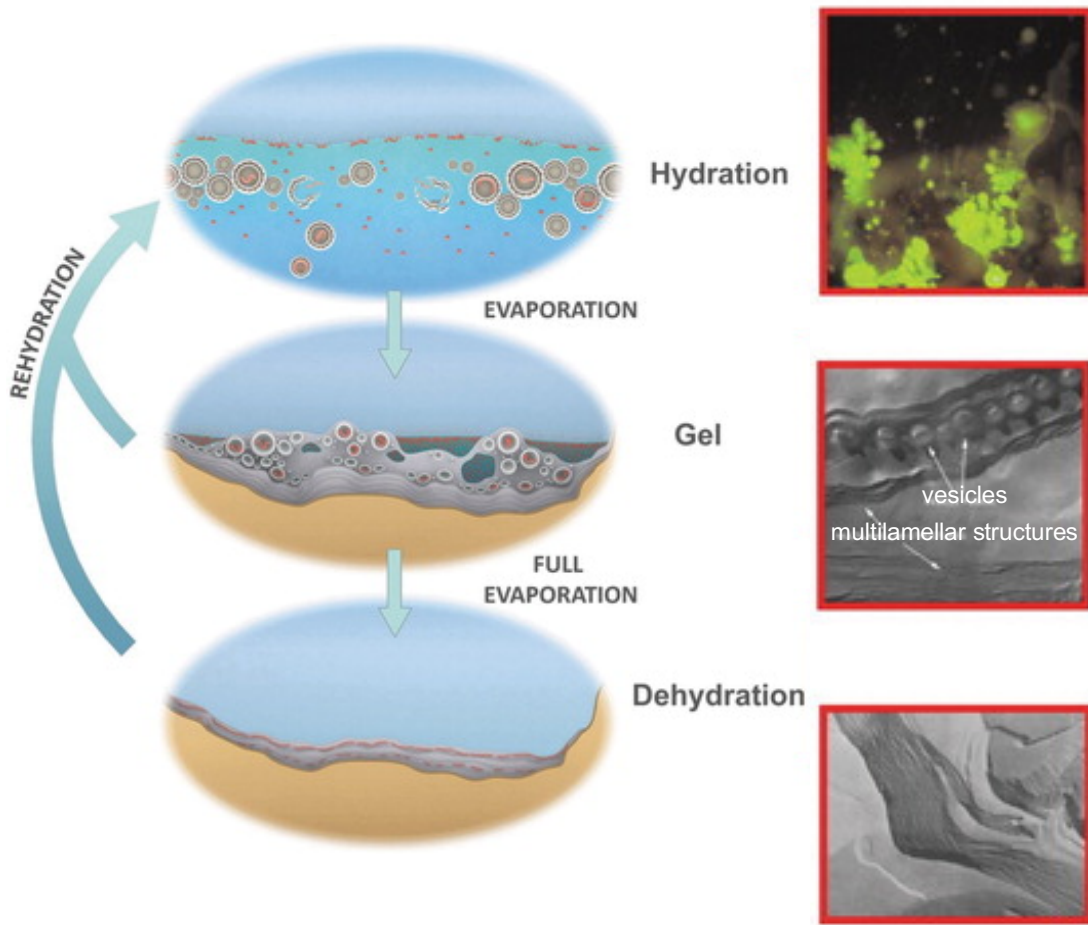


Figure 20: 'Wet-dry' cycles in natural hot spring pools generate three phases of lipid vesicle encapsulation: wet (vesicles and protocells), intermediate (lipid-polymer gel) and dry (concentrated lamellar film of fused lipids). Micrographs of these phases are shown on the right: phospholipid vesicles containing DNA stained with acridine orange under fluorescence (top right), freeze-fractured images of lipids in the gel phase (50% hydration) fusing from vesicles into lamellar structures (center right), and freeze-fractured dried out lipid lamellar structure made of phosphatidylcholine (bottom right). This figure was taken from Damer & Deamer (2020).

6.5.2 Multilamellar vesicles

As seen in Figure 8, section 5.1, lipid vesicles after one wet-dry cycle in the presence of RNA are made predominantly of multilamellar membranes and are still able to form in high concentrations of Ca^{2+} cations. One explanation for the relative stability of vesicles in a wet-dry cyclic environment containing RNA is that multilamellar structures form via a binding interaction similar to that observed in Black et al. (2013), but as full polymer strands interacting in the gel phase (Figure 20) instead of individual RNA monomers binding to vesicles. This would allow multiple lipid membranes to remain in close proximity upon rehydration, creating the multilamellar structures seen in Figure 8c. The effect of this process in the presence of cations is that the outermost membrane of the lipid vesicle is subjected to cation binding while the underlying membranes are protected and able to re-form membranes upon rehydration. This introduces an advantage for protocells with multiple membranes by providing additional layers of protection of the internal contents, and thus could partially explain reduced aggregation (i.e., increased stability of protocells) as seen in section 5.3.4, Figure 15. This ‘outer layer’ feature of primitive cell membranes is conserved in modern cells, known as the ‘cell envelope’ which has multiple layers of lipids as an outer barrier to environmental changes (Silhavy et al., 2010; Willdig & Helmann, 2021).

6.5.3 Effect of morphological differences on light absorbance

Light absorbance and light scattering are sensitive not only to the number of vesicles in solution and their degree of aggregation, but also to the morphology and size of those vesicles (Chong & Colbow, 1976). Lipid vesicles in the presence of RNA form larger vesicles with a larger internal volume of solution (Figure 8). The resulting size and shape of the vesicles is referred to as ‘osmotic swelling’, which is due to high concentrations of nucleic acids inside vesicles (Schrum et al.,

2010). Vesicles with larger internal volumes can allow more light to pass through them, which could contribute to the reduced amount of light absorbance and turbidity observed in Figure 14. However, given that RNA-lipid vesicles also demonstrate some resistance to aggregation via the formation of multilamellar structures, it is likely a combination of morphology and stability contributing to the reduced light absorbance reported in section 5.3.4.

6.5.4 Selection on the interaction between RNA and lipid vesicles.

The stabilizing role RNA plays on the formation of lipid vesicles is an important example of selection during the origin of cellular life. In this case, physical selection based on stability and molecular co-constraints provides a foundation for a transition to selection based on function interactions (which produce greater stability). For example, free floating RNA is inherently unstable in a dynamic chemical environment such as a hydrothermal system, but captured inside a protocell, it is protected from environmental stressors such as changes in pH and concentrations of ions. At the same time, RNA influences the morphology of the membrane, which contributes to increased stability of membranous vesicles. The interaction serves as a target for functional selection due to their mutually reinforcing chemical behavior. Their combination creates a robust macromolecular structure (a protocell) that provides a new stage for selection and evolution to operate on, beyond the physical characteristics of the individual molecules from which it is composed.

Protocells lack the molecular machinery to transcribe and translate genetic information to proteins, and provide directed synthesis, protection, regulation, and maintenance of cellular membranes as seen in modern cellular life (McDonald et al., 2015; Willdigg & Helmann, 2021; Koyiloth & Gummadi, 2022). However, it is possible that the genetic control of modern cell membranes is an amplification of a primitive effect, whereby nucleic acids (and perhaps other

polymers, peptides, and even RNA monomers alone (Black et al., 2013)) prevented membrane collapse. This served as a basis for functional selection (section 2.3) along the pathway towards Darwinian selection in a primitive version of evolution at the chemical level.

6.6 Role of iron in protocell formation

There appears to be a balance between the destabilizing effects of iron on lipid vesicles and the function that iron provides in catalyzing early prebiotic chemistry. Although Fe^{2+} was found to produce aggregation and destabilize lipid vesicles (but not as much as calcium), Fe^{2+} in the form of ferrous sulfate was observed to readily oxidize even under anaerobic conditions, likely due to trace amounts of O_2 in the anaerobic chamber, and produce salt precipitates, despite using a non-metal interacting buffer. Precipitates were an orange-red color, indicative of Fe(III)-oxyhydroxide formation. This demonstrates the extreme redox sensitivity of iron and suggests that in a natural prebiotic setting Fe^{2+} might have readily formed other compounds and precipitates, distinguishing its behavior from other metal cations like Ca^{2+} and Mg^{2+} . Fe^{2+} precipitates also contribute to the turbidity of solution, leading to 1) more experimental variability in results, where variable quantities of precipitates contribute to differences in light absorbance readings between replicates, and 2) potentially an over-estimation of the amount of turbidity caused by aggregation, given that some of the light absorbance is attributed to the precipitates. If a large proportion of Fe^{2+} free cations are binding with other compounds to produce salts, it is also possible that there is a lower concentration of iron in natural settings, reducing the impact iron could have on aggregation of lipid vesicles. Considering that a higher relative abundance of iron to calcium and magnesium is expected in the mineralogy of the martian surface (section 3.5), it is possible that Fe^{2+} does not pose as dramatic a selective barrier to emerging protocells as do other cations, such as calcium.

Furthermore, iron is thought to play an important role in RNA synthesis in primitive life (Hsiao et al., 2013; Okafor et al., 2017; Guth-Metzler et al., 2020), so one could speculate that an iron-based substrate could potentially have acted as a metal catalyst during early polymer formation. This requires extensive further investigation but provokes the question of when and how Fe^{2+} became important to the evolution of protocells, if it did not interact with membranes to the same extent as its ionic counterparts.

6.7 Research context

To summarize key previous investigations of conditions for protocell formation and aggregation relevant to this thesis research, Table 3 highlights key background research, areas this thesis research expands on, and novel contributions for future research in this area.

Table 3: Previous investigations of conditions for protocell formation and aggregation that this thesis research builds from, highlighting novel findings.

Previous work	This work	
	Overall trends found	Novelty
<ul style="list-style-type: none"> - Formation of protocells, sensitivity of fatty acid membranes to divalent cations, effect of pH on vesicle formation (Deamer et. al, 1982-2022) - Aggregation or ‘flocculation’ of protocells in salt water (Black et al. 2013) 	<ul style="list-style-type: none"> - Fe^{2+} destabilizes membrane vesicles, less than Ca^{2+}, but more than Mg^{2+} - Acidic pH reduces aggregation - Mixed-fatty acid membranes resist aggregation 	<ul style="list-style-type: none"> - Effect of Fe^{2+} on vesicle stability (with implications for Mars) - Vesicles made of a mosaic of fatty acids are more stable
<ul style="list-style-type: none"> - Individual nucleobases (monomers of RNA) bind to fatty acid membranes 	<ul style="list-style-type: none"> Vesicles that underwent wet-dry cycling and encapsulated RNA resisted aggregation 	<ul style="list-style-type: none"> - RNA polymers stabilize fatty acid membranes

<p>- Fatty acid membranes bound to nucleobases inhibit flocculation (aggregation in the presence of salt / Na⁺) (Black et al., 2013)</p>		<p>- Wet dry cycling in the presence of RNA produces large multilamellar vesicles</p>
<p>Methods for assessing vesicle stability and aggregation: fluorescent microscopy, dye permeability, UV-Vis spectrophotometry.</p>	<p>Aggregation and stability quantified by measuring light absorbance with spectrophotometry.</p>	<p>Using spectrophotometry for aggregation exceeded expectations and proved a useful approach for quantitatively comparing cation aggregation.</p>

7. Implications and Conclusions

7.1 Future work

The research presented in this thesis would benefit from continued consideration of how the planetary conditions on Mars would have affected the origin of life process hypothesized for hydrothermal settings. The conditions relevant to an origin of life process go far beyond habitability (Deamer et al., 2022) and could be investigated experimentally with respect to Mars. As pointed out in this work, Mars' iron-rich surface geochemistry could have produced a higher relative abundance of iron cations in prebiotic environments. Other factors such as lower temperatures, loss of surface water, and increasing UV radiation on Mars are also empirically testable and important for understanding the fate of protocell communities on Mars. Could a robust microbial martian colony have overcome these challenges, through chemical solutions that differed from those found on Earth? Future work investigating these factors would build a foundation for assessing how conducive Mars was to originating and sustaining life, as well as account for potentially divergent evolutionary trajectories for life on Mars.

Future experimental investigations following on from this research would strengthen the findings discussed in sections 5 and 6. Primarily, investigating where the RNA is located inside the protocells following a wet-dry cycle would be highly informative for understanding the role it plays. For example, it could be bound to the membranes themselves, indicating the stabilizing effect could be a result of RNA-lipid binding. Alternatively, if the RNA is free inside the protocells, this could imply that RNA-lipid co-stabilization is a general physical effect of co-localization. Such an investigation could be achieved with sophisticated fluorescent imaging techniques and increased environmental controls to engineer different interactions and observe their effects.

Repeating the experimental method outlined in section 4 to investigate vesicle aggregation in alkaline pH, temperatures above the phase transition of LA, including peptide polymers in wet-dry cycling, and with different relative abundances of Ca, Fe, and Mg would validate the robustness of the results of this research. Adding these variables would encompass more realistic conditions and build an understanding of the extent of experimental variation and the role of environmental conditions on vesicle stability. Additionally, increasing our knowledge of the conditions that affect vesicle stability allows for a better assessment of the importance of different geochemical compositions in hydrothermal settings for the evolution of early life.

Another interesting extension of this work is to consider the impact of iron on polymerization. It would be interesting to determine what iron salts are formed in hydrothermal pools, and whether they interact with individual amino acids and nucleobases during wet-dry cycling or RNA synthesis under anaerobic conditions. If iron either destabilizes protocells or forms salts in solution, knowing the compositions of the salts and their effects on prebiotic nucleic acid formation would help us understand how iron became so readily incorporated into early

biochemistry. Additionally, investigating how the presence of different metal cations affect the structural behavior of RNA and DNA could indicate their relationship in the origin of life. For example, Mg^{2+} largely impacts the folding and structure of RNA and DNA (Fisher et al., 2018; Xi et al., 2018), and allows nucleic acids to extend into linear strands in order for replication and extension to take place (a fundamental operation underlying all biology on Earth). Would Fe^{2+} affect the structure of RNA and DNA the same way or differently, given its unique atomic properties?

Peptides form from amino acids through condensation reactions during wet-dry cycles (section 2.4) and are readily available in planetary settings, both delivered by meteoritic infall (Damer & Deamer, 2020) and synthesized locally (Parker et al., 2014). Therefore, on the Hadean Earth 4 billion years ago, peptides could have been a more prebiotically plausible polymer than RNA precursors. Given that RNA synthesis is catalyzed by Fe^{2+} under anaerobic conditions (Hsiao et al., 2013; Okafor et al., 2017; Guth-Metzler et al., 2020), could Fe^{2+} have played a role in the synthesis of the earliest peptides as well? Or was it perhaps utilized for catalysis later in a more evolved set of chemical interactions and activated polymers? Future experiments could investigate the effect of iron on amino acid and RNA polymerization to explore whether Fe^{2+} , in comparison to other metal ions (Rode & Schwendinger, 1990), could act as a catalyst for early polymer formation.

Origin of life settings in natural systems display a huge diversity of combinatorial conditions. Testing the effect of individual variables on individual molecules is inherently unrealistic for understanding prebiotic environments (Deamer, 2022), and the origin of life field as a whole would benefit from new scientific approaches capable of characterizing complex systems, such as ‘messy chemistry’ approaches (advocated by Guttenberg et al. 2017). One aspect

of messy chemistry is the generation of diversity. Diversity is the platform that selection can act upon, and selection fuels directional organization such as in living processes. As discussed in section 6.5, selection can also act on the *interaction* between individual things, and in a natural setting with innumerable interactions contributing to messy chemistry, how selection acts on a network of interactions is a characteristic of origin of life settings that cannot be ignored. Complex systems and messy chemistry approaches could be important to conceiving and testing origin of life theories, because life is a process that organizes a messy background chemistry through selective and evolutionary processes.

7.2 An origin of life on Mars: Strategizing where we search for life based on the additional environmental challenges on Mars

Mars has a high surface expression of iron which could be both a selective barrier and a chemical evolutionary advantage for emerging protocell communities. The findings presented in this study imply that iron has a lesser effect on destabilizing vesicles than does calcium, which is significant for Mars' more iron-rich mineralogy. The observable difference between iron and other cations on protocell stability and function raises the possibility of divergence in the evolutionary trajectories for cellular life under early martian vs. terrestrial conditions, in terms of how conducive each planet was to the origin of life. As mentioned in the beginning of this section, there are additional environmental factors to consider that are different between Mars and Earth that would also affect the emergence of cellular life on Mars, which are discussed below and summarized in Figure 2 (introduction).

Early oxidation of Mars. Mars became oxidized ~3.5 Ga, whereas the GOE on Earth occurred ~2.4-2 Ga (Liu et al., 2021). The difference in size between Mars and Earth, as well as

the development of a biosphere in the case of Earth, contributed to this difference in timing for the onset of oxidizing conditions. Mars' reduced size, gravity, and loss of a dynamo-driven magnetic field made it more susceptible to atmospheric escape (Stevenson, 2001), resulting in more UV radiation and photo-oxidation at the surface. Other factors such as meteorite impacts in the presence of water (Deng et al., 2020) contributed to photo-oxidation processes. Regardless of the cause of the oxidation, if life was still getting started on Mars 3.5 Ga, it may not yet have had an evolutionary foothold to adapt under the short timescale of such a drastic change in planetary redox conditions between 3.5 and 3 Ga. The oxidizing planetary conditions would have affected both the environment life might have inhabited, but also the biochemistry itself, which is sensitive to redox states (e.g., carbon and nitrogen feedstocks of different organic molecules depending on oxidation state; Sasselov et al., 2020). If the increased surface expression of iron on Mars translated to an increased incorporation of or reliance upon iron for biological chemistry, there would have been increased pressure to adapt to the oxidizing conditions later in a planet's evolution given iron's high redox sensitivity.

Evaporating hydrosphere and increasing cation concentrations. Mars had a short-lived hydrosphere compared to Earth (Sasselov et al., 2020), which reduced the total surface water volume on Mars through time. In the context of this research, this implies that cation concentrations would have increased through time due to reduced volumes of water available to dissolve them. This would have been a challenge for emerging protocells sensitive to the adverse effects of cation-lipid binding. Salt (NaCl) is to be included in this assessment of cations on Mars, as there is extensive evidence of evaporites and salty brine remnants on Mars, the formation of which are linked to the loss of episodic surface water, contributing to a scenario where the concentration of salts and other cations at the surface continuously increased over time (King et

al., 2004). This is another geochemical constraint that could have provided a significant selective barrier for protocells on Mars, as salt has a dramatic osmotic effect on destabilizing membranes (see Appendix 4). These ionic challenges could be partially mitigated if life was emerging in volcanic hot springs rather than hydrothermal vents, as precipitation cycles provide a source of distilled freshwater in pools where protocells might be otherwise fighting cations for survival. As discussed in section 6.4, the concentrations at which the effect of aggregation becomes relevant are higher than observed in natural settings on Earth, perhaps serving as a healthy selective factor rather than a source of major destruction. However, during rapid loss of surface water on Mars, cation concentrations would be increasingly pushed towards mass aggregation, meaning that aggregation could have been a major selective barrier on Mars compared to Earth.

Compositions of primitive salts. In a primitive setting, the compositions of the lithophilically-derived salts may have been different than on present day Earth. Martian geology did not evolve highly felsic crusts capable of producing sodium- and phosphate-rich salts as on Earth, so it is possible that the salt composition on Mars reflects a more primitive atmosphere and source rock composition. Volcanic settings with acidic atmospheric conditions and mafic crustal compositions (Moore et al., 2010; Bullock et al., 2010) are thought to have led to widespread magnesium sulfate brines ($\text{MgSO}_4 \cdot \text{H}_2\text{O}$) ~3.7-2.9 Ga that we observe on Mars (Chipera & Vaniman, 2007). This is another important geochemical factor to consider for the origin of life on Mars, because although the effect of salt on protocell formation is well established (Milshteyn et al. 2018), the effect of plausible primitive salts on protocell formation is not. Additionally, building an understanding of whether there is a prebiotically plausible mechanism for protocells to combat high salt (Jordan et al., 2019) would be beneficial to understanding how life on Mars could have been shaped by high salt content at the surface.

Implications for space exploration. These additional challenges have implications for future exploration strategies seeking signs on ancient life on Mars. If life could not emerge and form strong footholds between 4 and 3.5 Ga, it may not have had the biological technology to adapt to rapidly changing planetary conditions that took place after 3.5-3 Ga and survive, let alone be later distributed from hot spring settings to inhabit littoral and lacustrine regions such as Jezero crater (Longo & Damer, 2020). This helps us to determine which locations on Mars will enable us to best assess whether life emerged on Mars, or how far prebiotic chemistry progressed, for future exploration endeavors. If life did not reach the ‘distribution phase’ during the planetary origin of life transition (Figure 3, section 2.1), then origin of life sites such as volcanic hot springs recognized in multiple locations on Mars (Michalski et al., 2017; Sasselov et al., 2020; Longo & Damer, 2020) would be the most strategic places to target for exploration, as they could host the first and last outposts of life on Mars. Life on Mars would have had a strong evolutionary incentive to retreat underground through the hydrothermal plumbing (Longo and Damer, 2020), and with great interest for searching for life in subterranean environments on Mars (Reichhardt, 2005), these locations provide a promising pathway forward.

7.3 Concluding remarks

All cations destabilize protocell membranes, but the relative extent of destabilization by different cations is determined by their unique atomic properties and interaction with water. The resistance of lipid membranes to cations in solution is greatly affected by the physical and chemical conditions in the local environment (e.g., temperature, pH, wet-dry cycling), which act as selective factors driving the co-evolution of membranes and functional polymers (e.g. RNA) to become protocell communities on the path toward becoming living cells.

There is a fundamental connection between geochemical settings and the biological chemistry that originates from them. For planets to develop life from an early surface prebiotic chemistry phase, sufficiently dynamic and combinatorically complex environments capable of driving selection must be sustained. Hydrothermal hot springs are an example of such settings that can accumulate but also mechanistically combine organic molecules into a living system through cycling and selection (e.g., cation exposure). The nature of this cyclic and selective environment is reflected and amplified by life today, which is inherently cyclic and evolves through the same selection mechanisms present in the chemical environment of life's origin. Life cannot be described by any particular suite of molecules or chemical reactions, but can be described by the selective, collaborative, combinatoric, and organizational processes that become integrated at the molecular level, that lead to the emergence of a new scale of reality beyond chemistry, that we call life.

References

- Abramov, O., & Kring, D. (2005). Impact-induced hydrothermal activity on early Mars. *Journal of Geophysical Research*, 110(E12). doi: 10.1029/2005je002453
- Ball, J.W., McCleskey, R.B., Nordstrom, D.K., Holloway, J.M., and Verplanck, P.L. (2002). Water-chemistry data for selected springs, geysers, and streams in Yellowstone National Park, Wyoming, 1999–2000, Open-File Report 02-382, U.S. Geological Survey, Boulder, CO.
- Barge, L., Flores, E., Baum, M., Vander Velde, D., & Russell, M. (2019). Redox and pH gradients drive amino acid synthesis in iron oxyhydroxide mineral systems. *Proceedings of the National Academy of Sciences*, 116(11), 4828-4833. doi:10.1073/pnas.1812098116
- Barge, L., Flores, E., Weber, J., Fraeman, A., Yung, Y., & VanderVelde, D. et al. (2022). Prebiotic reactions in a Mars analog iron mineral system: effects of nitrate, nitrite, and ammonia on amino acid formation. *Geochimica et Cosmochimica Acta*. doi: 10.1016/j.gca.2022.08.038
- Black, R., Blosser, M., Stottrup, B., Tavakley, R., Deamer, D., & Keller, S. (2013). Nucleobases bind to and stabilize aggregates of a prebiotic amphiphile, providing a viable mechanism for the emergence of protocells. *Proceedings of the National Academy of Sciences*, 110(33), 13272-13276. <https://doi.org/10.1073/pnas.1300963110>
- Blankenship, R. (2010). Early evolution of photosynthesis. *Plant Physiology*, 154(2), 434-438. doi: 10.1104/pp.110.161687
- Chipera, S., & Vaniman, D. (2007). Experimental stability of magnesium sulfate hydrates that may be present on Mars. *Geochimica et Cosmochimica Acta*, 71(1), 241-250. doi: 10.1016/j.gca.2006.07.044

- Cohen, I., & Marron, A. (2020). The evolution of universal adaptations of life is driven by universal properties of matter: energy, entropy, and interaction. *F1000research*, 9, 626. doi: 10.12688/f1000research.24447.3
- Crandall, J., Filiberto, J., Castle, N., Potter-McIntyre, S., Schwenzer, S., Olsson-Francis, K., & Perl, S. (2021). Habitability of martian noachian hydrothermal systems as constrained by a terrestrial analog on the Colorado Plateau. *The Planetary Science Journal*, 2(4), 138. doi: 10.3847/psj/ac053e
- Dalai, P., Ustriyana, P., & Sahai, N. (2018). Aqueous magnesium as an environmental selection pressure in the evolution of phospholipid membranes on early Earth. *Geochimica et Cosmochimica Acta*, 223, 216-228. doi: 10.1016/j.gca.2017.11.034
- Damer, B., & Deamer, D. (2020). The hot spring hypothesis for an origin of life. *Astrobiology*, 20(4), 429-452. doi: 10.1089/ast.2019.2045
- Deamer, D. (2022). Origins of life research: The conundrum between laboratory and field simulations of messy environments. *Life*, 12(9), 1429. doi: 10.3390/life1209142
- Deamer, D., & Dworkin, J. (2005). Chemistry and physics of primitive membranes. *Prebiotic Chemistry*, 1-27. doi: 10.1007/b136806
- Deamer, D., Cary, F., & Damer, B. (2022). Urability: A property of planetary bodies that can support an origin of life. *Astrobiology*, 10.1089/ast.2021.0173.
- Deamer, D., Damer, B., & Kompanichenko, V. (2019). Hydrothermal chemistry and the origin of cellular life. *Astrobiology*, 19(12), 1523-1537. doi: 10.1089/ast.2018.1979
- Dehouck, E., Gaudin, A., Chevrier, V., & Mangold, N. (2016). Mineralogical record of the redox conditions on early Mars. *Icarus*, 271, 67-75.

- Deng, Z., Moynier, F., Villeneuve, J., Jensen, N., Liu, D., Cartigny, P. et al. (2020). Early oxidation of the martian crust triggered by impacts. *Science Advances*, 6(44). doi: 10.1126/sciadv.abc4941
- Dudev, T., & Lim, C. (2013). Importance of metal hydration on the selectivity of Mg^{2+} versus Ca^{2+} in magnesium ion channels. *Journal of the American Chemical Society*, 135(45), 17200-17208. doi: 10.1021/ja4087769
- Earle, S. (2020). *Physical Geology*, 2nd ed., pp. 156-159, Chapter 5 Weathering and Soil. BCcampus Open Education.
- Filiberto, J., & Schwenzer, S. (2013). Alteration mineralogy of Home Plate and Columbia Hills-Formation conditions in context to impact, volcanism, and fluvial activity. *Meteoritics & Planetary Science*, 48(10), 1937-1957. <https://doi.org/10.1111/maps.12207>
- Fischer, N. M., Polêto, M. D., Steuer, J., Spoel, D. (2018) Influence of Na^+ and Mg^{2+} ions on RNA structures studied with molecular dynamics simulations. *Nucleic Acids Research*, Volume 46, Issue 10. Pages 4872–4882. <https://doi.org/10.1093/nar/gky221>
- Fornari, D., & Embley, R. (2013). Tectonic and volcanic controls on hydrothermal processes at the mid-ocean ridge: an overview based on near-bottom and submersible studies. *Seafloor hydrothermal systems: physical, chemical, biological, and geological interactions*, 1-46. doi: 10.1029/gm091p0001
- Forterre, P., Filée, J, Myllykallio, H. (2000-2013). Origin and Evolution of DNA and DNA Replication Machineries. In: Madame Curie Bioscience Database [Internet]. Austin (TX): Landes Bioscience. Available from: <https://www.ncbi.nlm.nih.gov/books/NBK6360/>
- Frank, A., Grinspoon, D., & Walker, S. (2022). Intelligence as a planetary scale process. *International Journal of Astrobiology*, 21(2), 47-61. doi: 10.1017/s147355042100029x

- Furukawa, H., & Walker, S. (2018). Major transitions in planetary evolution. The 2018 Conference on Artificial Life. doi: 10.1162/isal_a_00024
- Gavette, J. M., Stoop, M., Hud, N. V., Krishnamurthy, R. (2016) RNA–DNA Chimeras in the Context of an RNA World Transition to an RNA/DNA World. *Angewandte Chemie, Communications, Chemical Evolution*. 55, 13204-13209.
- Gellert, R., Rieder, R., Anderson, R., Brückner, J., Clark, B., Dreibus, G. et al. (2004). Chemistry of rocks and soils in Gusev Crater from the alpha particle x-ray spectrometer. *Science*, 305(5685), 829-832. <https://doi.org/10.1126/science.1099913>
- Gözen, I., Köksal, E., Pöldsalu, I., Xue, L., Spustova, K., Pedrueza-Villalmanzo, E. et al. (2022). Protocells: milestones and recent advances. *Small*, 18(18), 2106624. doi: 10.1002/sml.202106624
- Guth-Metzler, R., Bray, M., Frenkel-Pinter, M., Suttapitugsakul, S., Montllor-Albalade, C., Bowman, J. et al. (2020). Cutting in-line with iron: ribosomal function and non-oxidative RNA cleavage. *Nucleic Acids Research*, 48(15), 8663-8674. <https://doi.org/10.1093/nar/gkaa586>
- Guttenberg, N., Virgo, N., Chandru, K., Scharf, C., & Mamajanov, I. (2017). Bulk measurements of messy chemistries are needed for a theory of the origins of life. *Philosophical Transactions of The Royal Society A: Mathematical, Physical and Engineering Sciences*, 375(2109), 20160347. doi: 10.1098/rsta.2016.0347
- Halliday, A., Wänke, H., Birck, J., & Clayton, R. (2001). The accretion, composition, and early differentiation of Mars. *Space Science Reviews*, 96(1/4), 197-230. <https://doi.org/10.1023/a:1011997206080>

- Hsiao, C., Chou, I., Okafor, C., Bowman, J., O'Neill, E., Athavale, S. et al. (2013). RNA with iron (II) as a cofactor catalyses electron transfer. *Nature Chemistry*, 5(6), 525-528. doi: 10.1038/nchem.1649
- Jordan, S.F. and Rammu, H. and Zheludev, I.N. and Hartley, Andrew and Marechal, Amandine and Lane, N. (2019) Promotion of protocell self-assembly from mixed amphiphiles at the origin of life. *Nature Ecology & Evolution*, ISSN 2397-334X.
- Kaplan, J., & Ward, D. (2013). The essential nature of iron usage and regulation. *Current Biology*, 23(22), 2325. <https://doi.org/10.1016/j.cub.2013.10.059>
- King, P., Lescinsky, D., & Nesbitt, H. (2004). The composition and evolution of primordial solutions on Mars, with application to other planetary bodies. *Geochimica et Cosmochimica Acta*, 68(23), 4993-5008. doi: 10.1016/j.gca.2004.05.036
- Koyiloth, M., & Gummadi, S. (2022). Regulation and functions of membrane lipids: Insights from *Caenorhabditis elegans*. *BBA Advances*, 2, 100043. doi: 10.1016/j.bbadv.2022.100043
- Kriegler, S., Herzog, M., Oliva, R., Gault, S., Cockell, C., & Winter, R. (2021). Structural responses of model biomembranes to Mars-relevant salts. *Physical Chemistry Chemical Physics*, 23(26), 14212-14223. doi: 10.1039/d1cp02092g
- Langmuir, C., Humphris, S., Fornari, D., Van Dover, C., Von Damm, K., & Tivey, M. et al. (1997). Hydrothermal vents near a mantle hot spot: the Lucky Strike vent field at 37°N on the Mid-Atlantic Ridge. *Earth And Planetary Science Letters*, 148(1-2), 69-91. doi: 10.1016/s0012-821x(97)00027-7
- Liu, J., Michalski, J., Tan, W., He, H., Ye, B., & Xiao, L. (2021). Anoxic chemical weathering under a reducing greenhouse on early Mars. *Nature Astronomy*, 5(5), 503-509. <https://doi.org/10.1038/s41550-021-01303-5>

- Longo, A., & Damer, B. (2020). Factoring origin of life hypotheses into the search for life in the solar system and beyond. *Life*, 10(5), 52. doi: 10.3390/life10050052
- McCollom, T., Ritter, G., & Simoneit, B. (1999). Origins of life and evolution of the biosphere, 29(2), 153-166. doi: 10.1023/a:1006592502746
- McDonald, C., Jovanovic, G., Ces, O., & Buck, M. (2015). Membrane stored curvature elastic stress modulates recruitment of maintenance proteins PspA and Vipp1. *Mbio*, 6(5). doi: 10.1128/mbio.01188-15
- McSween, H., Arvidson, R., Bell, J., Blaney, D., Cabrol, N., Christensen, P. et al. (2004). Basaltic rocks analyzed by the Spirit rover in Gusev Crater. *Science*, 305(5685), 842-845. <https://doi.org/10.1126/science.3050842>
- Michalski, J., Dobreá, E., Niles, P., & Cuadros, J. (2017). Ancient hydrothermal seafloor deposits in Eridania basin on Mars. *Nature Communications*, 8(1). <https://doi.org/10.1038/ncomms15978>
- Michalski, J., Onstott, T., Mojzsis, S., Mustard, J., Chan, Q., Niles, P., & Johnson, S. (2017). The martian subsurface as a potential window into the origin of life. *Nature Geoscience*, 11(1), 21-26. <https://doi.org/10.1038/s41561-017-0015-2>
- Milshteyn, D., Damer, B., Havig, J., & Deamer, D. (2018). Amphiphilic compounds assemble into membranous vesicles in hydrothermal hot spring water but not in seawater. *Life*, 8(2), 11. doi: 10.3390/life8020011
- Mohan, C. Calbiochem®: A guide for the preparation and use of buffers in biological systems.
- Moore, J., Bullock, M., Newsom, H., & Nelson, M. (2010). Laboratory simulations of Mars evaporite geochemistry. *Journal of Geophysical Research*, 115(E6). doi: 10.1029/2008je003208

- Morris, R., Ruff, S., Gellert, R., Ming, D., Arvidson, R., Clark, B. et al. (2010). Identification of carbonate-rich outcrops on Mars by the Spirit rover. *Science*, 329(5990), 421-424.
<https://doi.org/10.1126/science.1189667>
- Okafor, C., Lanier, K., Petrov, A., Athavale, S., Bowman, J., Hud, N., & Williams, L. (2017). Iron mediates catalysis of nucleic acid processing enzymes: support for Fe (II) as a cofactor before the great oxidation event. *Nucleic Acids Research*, 45(7), 3634-3642. doi: 10.1093/nar/gkx171
- Outten, F., & Theil, E. (2009). Iron-based redox switches in biology. *Antioxidants & Redox Signaling*, 11(5), 1029-1046. doi: 10.1089/ars.2008.2296
- Parker, E., Cleaves, J., Burton, A., Glavin, D., Dworkin, J., Zhou, M. et al. (2014). Conducting Miller-Urey experiments. *Journal of Visualized Experiments*, (83). doi: 10.3791/51039
- Reichhardt, T. (2005). Going underground. *Nature*, 435(7040), 266-267. doi: 10.1038/435266a
- Rode, B., & Schwendinger, M. (1990). Copper-catalyzed amino acid condensation in water - a simple possible way of prebiotic peptide formation. *Origins of Life and Evolution of the Biosphere*, 20(5), 401-410. doi: 10.1007/bf01808134
- Rouxel, O., Bekker, A., & Edwards, K. (2005). Iron isotope constraints on the Archean and Paleoproterozoic ocean redox state. *Science*, 307(5712), 1088-1091. doi: 10.1126/science.1105692
- Ruff, S., Campbell, K., Van Kranendonk, M., Rice, M., & Farmer, J. (2020). The case for ancient hot springs in Gusev Crater, Mars. *Astrobiology*, 20(4), 475-499. doi: 10.1089/ast.2019.2044

- Rushdi, A., & Simoneit, B. (2006). Abiotic condensation synthesis of glyceride lipids and wax esters under simulated hydrothermal conditions. *Origins of Life and Evolution of Biospheres*, 36(2), 93-108. doi: 10.1007/s11084-005-9001-6
- Sasselov, D., Grotzinger, J., & Sutherland, J. (2020). The origin of life as a planetary phenomenon. *Science Advances*, 6(6), eaax3419. <https://doi.org/10.1126/sciadv.aax3419>
- Schrum, J., Zhu, T., & Szostak, J. (2010). The origins of cellular life. *Cold Spring Harbor Perspectives in Biology*, 2(9), a002212-a002212. doi: 10.1101/cshperspect.a002212
- Shi, R., Zhao, Z., Huang, X., Wang, P., Su, Y., Sai, L. et al. (2021). Ground-state structures of hydrated calcium ion clusters from comprehensive genetic algorithm search. *Frontiers In Chemistry*, 9. doi: 10.3389/fchem.2021.637750
- Silhavy, T., Kahne, D., & Walker, S. (2010). The bacterial cell envelope. *Cold Spring Harbor Perspectives in Biology*, 2(5), a000414-a000414. doi: 10.1101/cshperspect.a000414
- Stevenson, D. (2001). Mars' core and magnetism. *Nature*, 412(6843), 214-219.
<https://doi.org/10.1038/35084155>
- Taylor, S. R., & McLennan, S. (2009). *Planetary crusts: their composition, origin, and evolution* (Vol. 10). Cambridge University Press.
- Van Kranendonk, M., Baumgartner, R., Cady, S., Campbell, K., Damer, B., Deamer, D., Djokic, T., Gangidine, A., Ruff, S., & Walter, M. R. (2021). Terrestrial hydrothermal fields and the search for life in the solar system. *Bulletin of the AAS*, 53(4).
<https://doi.org/10.3847/25c2cfcb.a3a646ab>
- Wade, M., Agresti, D., Wdowiak, T., Armendarez, L., & Farmer, J. (1999). A Mössbauer investigation of iron-rich terrestrial hydrothermal vent systems: lessons for Mars exploration. *Journal of Geophysical Research: Planets*, 104(E4), 8489-8507. doi: 10.1029/1998je900049

Willdigg, J., & Helmann, J. (2021). Mini review: bacterial membrane composition and its modulation in response to stress. *Frontiers In Molecular Biosciences*, 8. doi: 10.3389/fmolb.2021.634438

Wu, L., Brucker, R., Beard, B., Roden, E., & Johnson, C. (2013). Iron isotope characteristics of hot springs at Chocolate Pots, Yellowstone National Park. *Astrobiology*, 13(11), 1091-1101. doi: 10.1089/ast.2013.0996

Xi, K., Wang, F. H., Xiong, G., Zhang, Z. L., Tan, Z. J. (2018). Competitive binding of Mg²⁺ and Na⁺ ions to nucleic acids: from helices to tertiary structures. *Biophys J.* 114(8):1776-1790. doi: 10.1016/j.bpj.2018.03.001

Zuber, M. (2001). The crust and mantle of Mars. *Nature*, 412(6843), 220-227.

<https://doi.org/10.1038/35084163>

Appendices

Table of contents

Appendix 1: Experimental protocol and material list for measuring vesicle aggregation with spectrophotometry	73
Materials	73
Protocol	73
Appendix 2: Data for individual experiments	77
Lauric acid and glycerol monolaurate (LAGML) vesicles	77
Lauric acid and glycerol monolaurate (LAGML) vesicles under acidic conditions	79
Capric acid and glycerol monolaurate (CAGML) vesicles	80
Lauric acid (LA) vesicles	81
Lauric and capric (LACA) vesicles	82
Lauric acid and glycerol monolaurate vesicles with RNA captured inside (RNA-LAGML)	83
Appendix 3: Ionic compositions of hot springs vs. seawater, implications for the role of salt in protocell assembly	84
Appendix 4: Spectrophotometer wavelength justification	85

Appendix 1: Experimental protocol and material list for measuring vesicle aggregation with spectrophotometry

Materials

Triethanolamine (TEA) buffer, pH 7.5 (100 mM stock)	Magnesium sulfate (MgSO_4)
2-ethanesulfonic acid (MES) buffer, pH 5.5 (100 mM stock)	Ferrous sulfate (FeSO_4)
18 M Ω Milli-Q water	Ferrous ammonium sulfate ($\text{Fe}(\text{NH}_4)_2(\text{SO}_4)_2 \cdot 6\text{H}_2\text{O}$)
Lauric acid ($\text{C}_{12}\text{H}_{24}\text{O}_2$)	Ferric ammonium sulfate ($\text{Fe}(\text{NH}_4)(\text{SO}_4)_2 \cdot 12\text{H}_2\text{O}$)
Capric acid ($\text{C}_{10}\text{H}_{20}\text{O}_2$)	Ammonium sulfate ($(\text{NH}_4)_2\text{SO}_4$)
Glycerol monolaurate ($\text{C}_{15}\text{H}_{30}\text{O}_4$)	Nitrogen gas (N_2)
Calcium chloride (CaCl_2)	Acridine orange ($\text{C}_{17}\text{H}_{19}\text{N}_3$)
Spectrophotometer (UV-1600PC UV-VIS, UEE1409033)	Microscope (Olympus BX43)
Controlled atmosphere chamber (Plas Labs model 855)	Oxygen gas detector by Forensics (detection range 0-30% with 0.1% resolution, Accuracy $\pm 5\%$ F.S.)

Protocol

Anaerobic chamber set-up

A controlled atmosphere chamber was used to create an anaerobic environment under nitrogen gas, where oxygen levels were controlled (0.0%VOL O_2). To prepare the chamber, nitrogen was flushed through the chamber ~23 times. The intended method for the chamber is to flush with 85% N_2 , 10% H_2 , 5% CO_2 9 times, followed by an additional drying step to clear residual oxygen. This would increase the temperature to 37 °C so residual oxygen forms condensation catalyzed by palladium pellets, which is then drying and removed by the chamber's drying train. This gas

composition was not obtainable (largely due to sociopolitical issues surrounding hydrogen gas during the war on Ukraine), so residual oxygen was not completely cleared but the additional ~14 flushing cycles with N₂ helped. All equipment needed for the experiments, including the spectrophotometer was contained inside the chamber prior to flushing, with caps removed to release any O₂. Solids were weighed and added to vials prior to entry into the chamber. Buffers were vigorously bubbled with nitrogen (3 minutes) prior to entry into the chamber to remove any dissolved oxygen. After bubbling a rubber stopper was placed on the buffer flasks immediately. Once oxygen was nearly all removed from the chamber (<1%VOL O₂), the rubber stopper was removed, so any residual gaseous O₂ could be removed in subsequent flushing steps.

Vesicle and cation solution preparation

1. Prepare a 10 mM vesicle stock solution (of LAGML, CAGML, LA, LACA, LAGML pH5.5) as described below (Table 1 from Section 4):
 - a) Weigh out solids (LA, GML, CA) needed for a 100 mM solution in 10mL
 - b) Add 10 mL of TEA (or MES for LAGML pH5.5 experiment) to the pre-weighed solids once inside anaerobic chamber and ready for analysis
 - c) Warm to ~40 °C, and vortex for 30 seconds
 - d) Dilute the 100 mM vesicle solution in buffer 1 in 10 to make a 10 mM vesicle solution
 - e) Warm to ~40 °C, and vortex for 30 seconds. Keep warm in hot bath during experiments

Table 1 (repeated): Vesicle preparation reference key, where lipids were prepared for aggregation experimentation to make vesicles composed of various mixtures of lauric acid (LA), capric acid (CA), glycerol monolaurate (GML), and RNA in buffer.

‘LAGML’	‘CAGML’	‘LAGML (acidic)’	‘LA’	‘LACA’	‘RNA-LAGML’
Lauric acid (LA, 12 carbons) and glycerol monolaurate (GML) (1:1 by weight) in 10 mM TEA pH 7.5	Capric acid (CA, 10 carbons) and glycerol monolaurate (GML) (1:1 by weight) in 10 mM TEA pH 7.5	LAGML in 10 mM MES pH 5.5	Pure LA in 10 mM TEA pH 7.5	LA and CA (1:1 by weight) in 10 mM TEA pH 7.5	LAGML and yeast RNA in a 4:1 ratio in 10 mM TEA pH 7.5, subjected to 1 wet-dry cycle.

2. Dilute the 100 mM stock solution (1 in 10) of TEA pH 7.5 (or MES for LAGML pH 5.5 experiment) in 18 MΩ Milli-Q water to make 10 mM buffer
3. Prepare 10 mL of 100 mM cation solutions
 - a) Weigh out solids (0.1109 g CaCl₂, 0.27801 g FeSO₄, 0.120366 g MgSO₄, 0.39215 g Fe(NH₄)₂(SO₄)₂, 0.48225 g FeNH₄(SO₄)₂, 0.13214 g (NH₄)₂SO₄).
 - b) Add 10 mL of TEA (or MES for LAGML pH 5.5 experiment) to the pre-weighed solids once inside anaerobic chamber and ready for analysis
 - c) Warm to ~40 °C and briefly vortex to mix (~10 seconds). Keep warm in hot bath during experiments.

RNA-LAGML vesicle solution preparation

4. Weigh 0.06 g LAGML and 0.015 g RNA solids (4:1 ratio by weight) and place in a test tube
5. Add 5 mL TEA buffer pH 7.5 to make a 50 mM LAGML + RNA solution.

6. Warm to ~ 40 °C and vortex for 1 minute
7. Transfer solution to a beaker and allow the liquid to evaporate on a hot plate until only a dry film remains.
8. Once inside the anaerobic chamber, add 25 mL of TEA buffer to the dehydrated film, immediately prior to experimentation. This is now a 10 mM LAGML + RNA solution.
9. Warmed to ~ 40 °C and mix by pipetting up and down until the solution appears homogeneous.

Spectrophotometry

10. Set spectrophotometer to 400 nm
11. Add 2 mL of 10 mM vesicle solution to a 1 cm cuvette/spectrophotometer cell, take a reading as a standard
12. For each sample, titrate in 5 μ L of the prepared cation solution to the cell, mixing by pipetting up and down ~ 5 times, take a spectrophotometry reading. Do 5 μ L increments until you reach a total cation volume addition of 60 μ L
13. Begin titrating at 10 μ L increments after you have reached 60 μ L total cation solution added to the cuvette
14. Allow the sample to sit for ~ 2 minutes so that aggregation can occur, and movement of suspended particles slows, then take a spectrophotometry reading
15. Repeat this procedure (steps 10-13) three times (triplicate experiments) for each cation in LAGML, CAGML, LA, LACA, LAGML pH 5.5, and RNA-LAGML experiments.

Note: Take a temperature reading before every experiment, and throughout experimentation/as soon as a temperature change is noticed. Two temperature sensors were inside the chamber and an average of the two was taken as the temperature reading. In this research, average temperature inside the chamber across all experiments was 86.4 °F and fluctuated by +/- 10 °F due to the heat generated by apparatus inside the chamber (spectrophotometer and hot plate).

Appendix 2: Data for individual experiments

Replicate data

Each experiment in Figures 21-26, and in section 5 (Figures 10-15), was performed in triplicate, meaning each experiment was repeated three times with a new sample each time. For example, in Figure 21 the pink dotted lines represent the three Mg²⁺ LAGML experiments, which were averaged to produce the solid pink line. This means each experiment was a true replicate, rather than replicate analysis of each sample, which both increases the robustness of the results and encompasses the natural variability between replicate samples.

Natural variability of experimental data

Aggregation is a physical phenomenon and samples are subject to a large degree of natural heterogeneity. This results in inflated uncertainty margins and variability in the plotted results displayed in this appendix and section 5. Given these uncertainties, absolute reproducibility is unlikely for aggregation studies; however, the observed relationship between different cations and their effect on aggregation is expected to be generally reproducible. Quantifying aggregation with spectrophotometry exceeded our expectations and proved a useful approach for quantitatively comparing cation aggregation moving forward.

Lauric acid and glycerol monolaurate (LAGML) vesicles

Vesicles made of lauric acid and glycerol monolaurate (LAGML) were the primary vesicle compositions used to explore the effect of calcium, iron, and magnesium on aggregation. LAGML solutions served as a reference point for the effect of other variables such as pH, inclusion of capric acid (CA), and RNA encapsulation. Figure 21 displays the increase in absorbance readings (i.e., aggregation) of LAGML vesicles in the presence of calcium, iron, and magnesium cations.

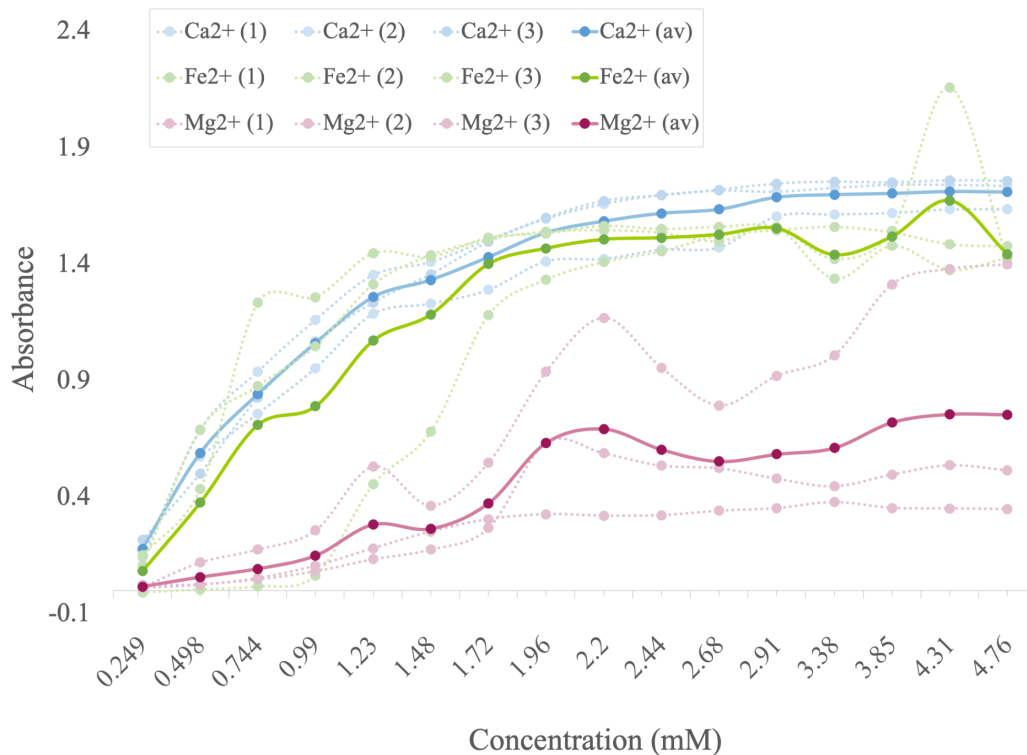


Figure 21: Light absorbance of LAGML lipid vesicle solutions in near-neutral pH (7.5) with increasing cation concentrations. High absorbance readings reflect high amounts of aggregation and unfavorable conditions for protocell formation. Dotted lines represent triplicate samples, solid lines represent the average of triplicates. Samples were analyzed using spectrophotometry at 400 nm under anaerobic conditions. LAGML solutions were 10 mM in concentration, and cation concentrations between 0-4.76 mM. Fe²⁺ samples were prepared with ferrous sulfate (FeSO₄), Ca²⁺ with calcium chloride (CaCl₂), and Mg²⁺ with magnesium sulfate (MgSO₄).

Lauric acid and glycerol monolaurate (LAGML) vesicles under acidic conditions

Figure 22 displays the increase in absorbance readings (i.e., aggregation) of LAGML vesicles under acidic conditions in the presence of calcium, iron, and magnesium cations.

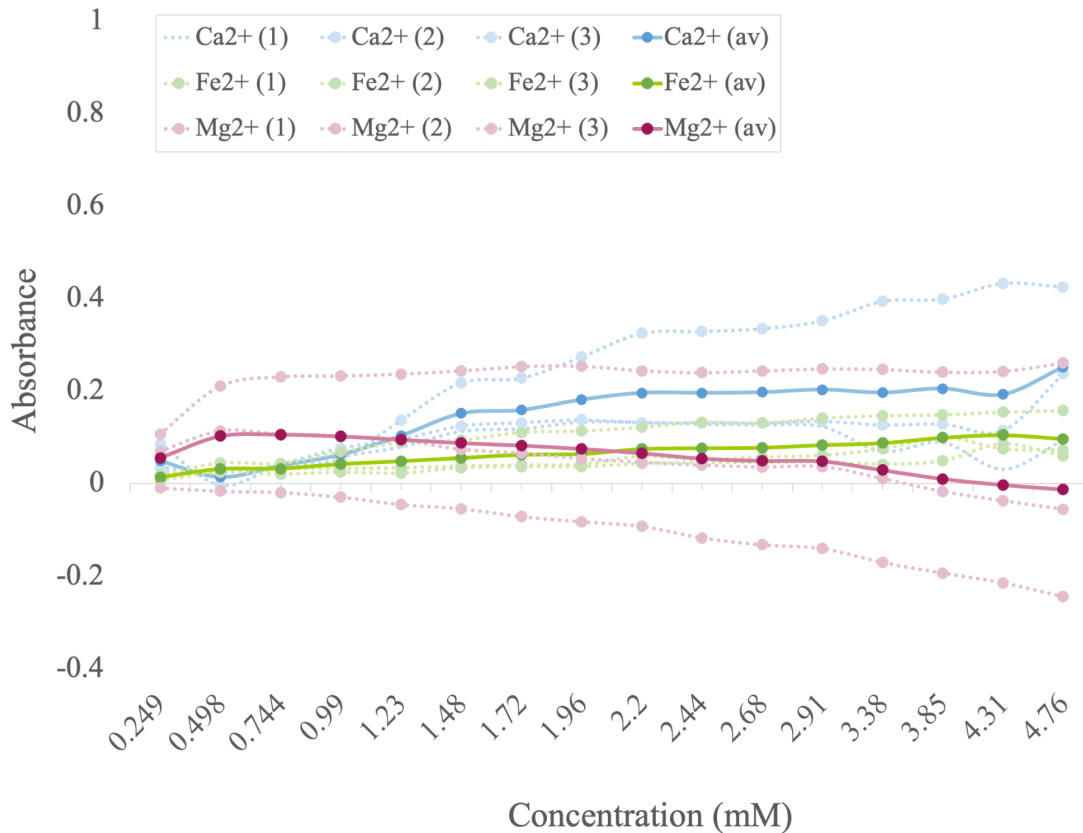


Figure 22: Light absorbance of LAGML lipid vesicle solutions in acidic pH (5.5) with increasing cation concentrations. High absorbance readings reflect high amounts of aggregation and unfavorable conditions for protocell formation. Dotted lines represent triplicate samples, solid lines represent the average of triplicates. Samples were analyzed using spectrophotometry at 400 nm under anaerobic conditions. LAGML solutions were 10 mM in concentration, and cation concentrations between 0-4.76 mM. Fe²⁺ samples were prepared with ferrous sulfate (FeSO₄), Ca²⁺ with calcium chloride (CaCl₂), and Mg²⁺ with magnesium sulfate (MgSO₄).

Capric acid and glycerol monolaurate (CAGML) vesicles

Figure 23 displays the increase in absorbance readings (i.e., aggregation) of CAGML vesicles in the presence of calcium, iron, and magnesium cations.

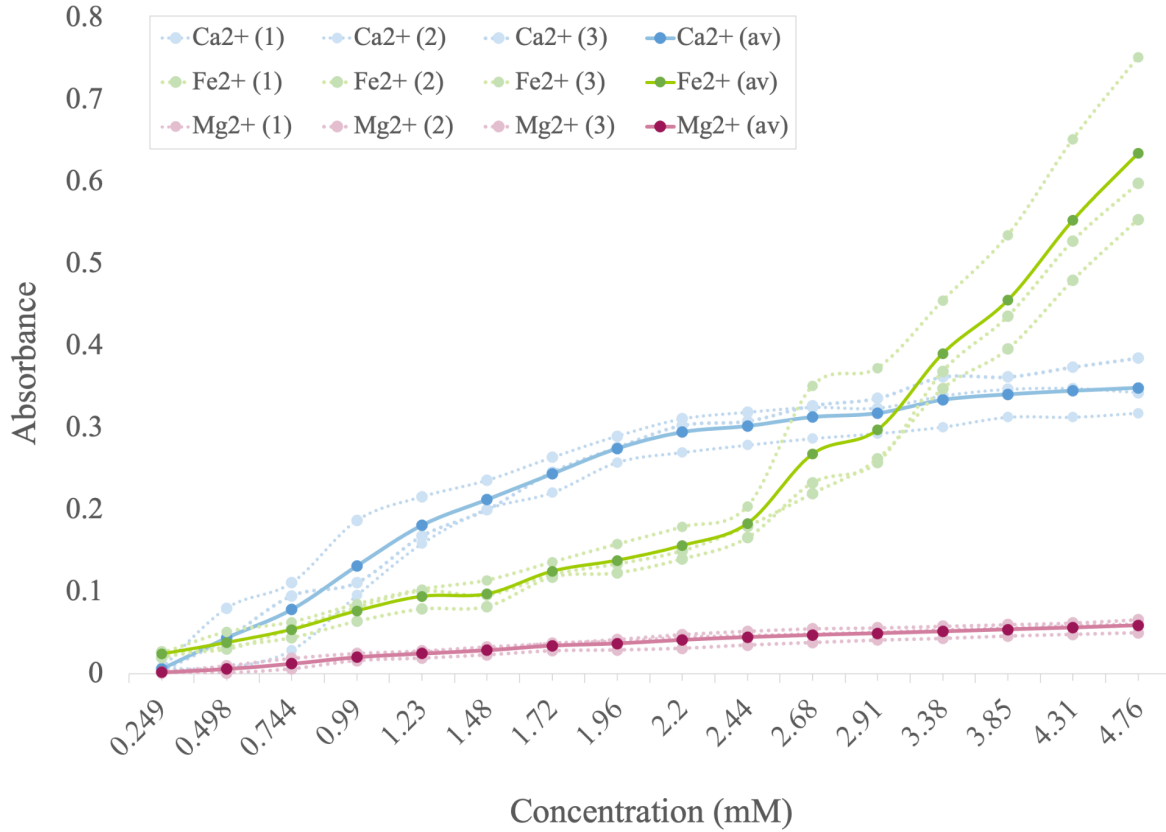


Figure 23: Light absorbance of CAGML lipid vesicle solutions with increasing cation concentrations, pH 7.5. High absorbance readings reflect high amounts of aggregation and unfavorable conditions for protocell formation. Dotted lines represent triplicate samples, solid lines represent the average of triplicates. Samples were analyzed using spectrophotometry at 400 nm under anaerobic conditions. LAGML solutions were 10 mM in concentration, and cation concentrations between 0-4.76 mM. Fe²⁺ samples were prepared with ferrous sulfate (FeSO₄), Ca²⁺ with calcium chloride (CaCl₂), and Mg²⁺ with magnesium sulfate (MgSO₄).

Lauric acid (LA) vesicles

Figure 24 displays the increase in absorbance readings (i.e., aggregation) of pure LA vesicles in the presence of calcium, iron, and magnesium cations.

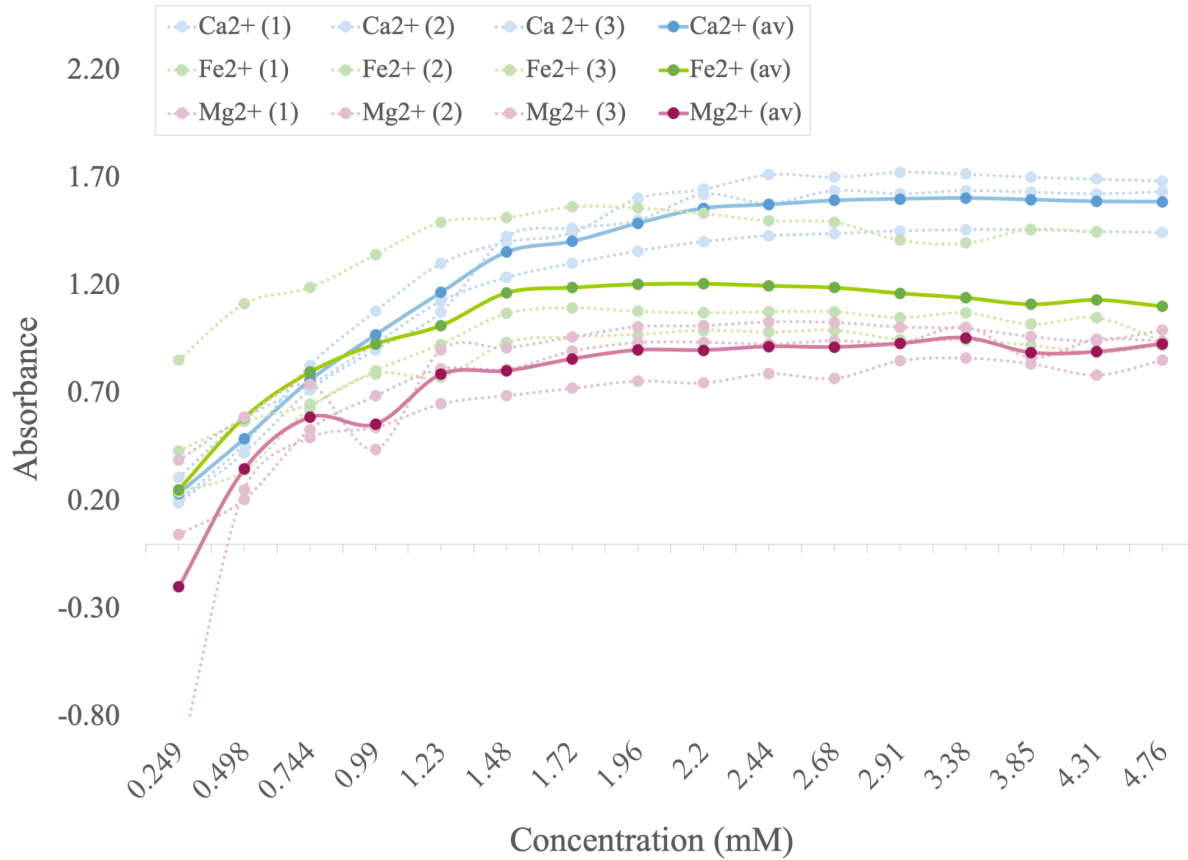


Figure 24: Light absorbance of LA lipid vesicle solutions with increasing cation concentrations, pH 7.5. High absorbance readings reflect high amounts of aggregation and unfavorable conditions for protocell formation. Dotted lines represent triplicate samples, solid lines represent the average of triplicates. Samples were analyzed using spectrophotometry at 400 nm under anaerobic conditions. LAGML solutions were 10 mM in concentration, and cation concentrations between 0-4.76 mM. Fe²⁺ samples were prepared with ferrous sulfate (FeSO₄), Ca²⁺ with calcium chloride (CaCl₂), and Mg²⁺ with magnesium sulfate (MgSO₄).

Lauric and capric (LACA) vesicles

Figure 25 displays the increase in absorbance readings (i.e., aggregation) of LACA vesicles in the presence of calcium, iron, and magnesium cations.

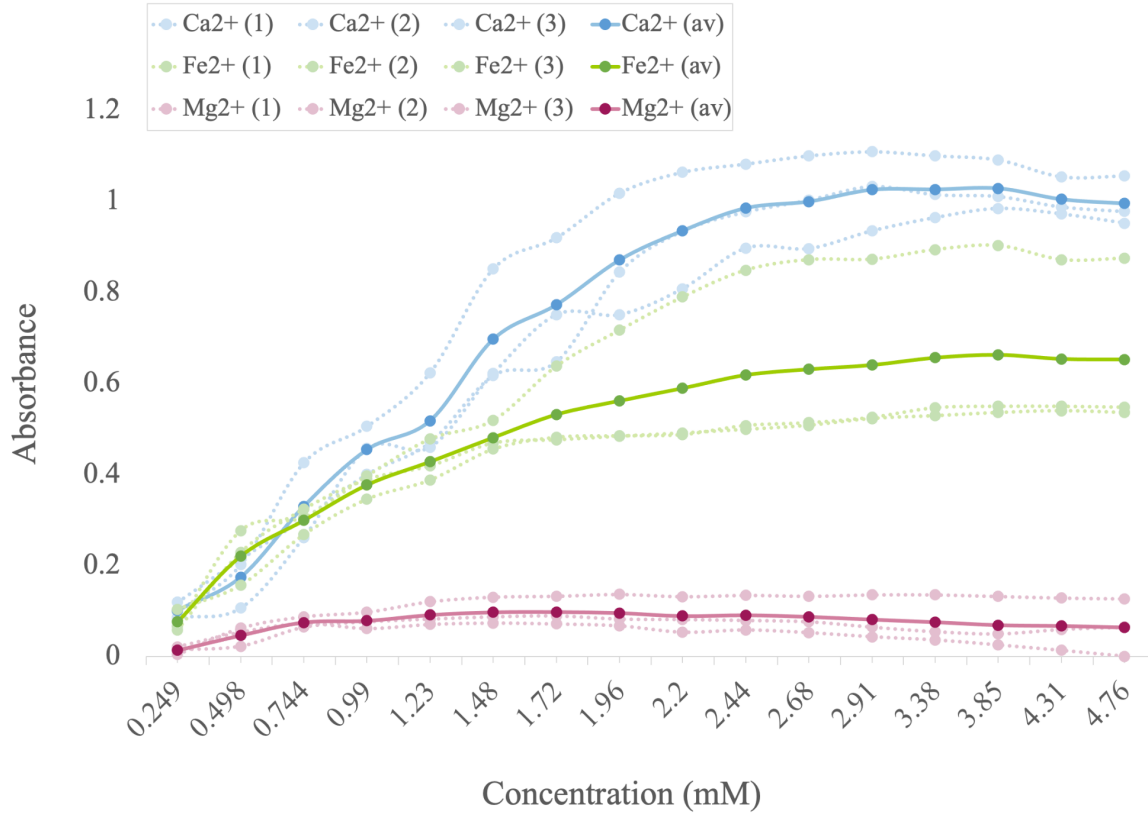


Figure 25: Light absorbance of LA lipid vesicle solutions with increasing cation concentrations, pH 7.5. High absorbance readings reflect high amounts of aggregation and unfavorable conditions for protocell formation. Dotted lines represent triplicate samples, solid lines represent the average of triplicates. Samples were analyzed using spectrophotometry at 400 nm under anaerobic conditions. LAGML solutions were 10 mM in concentration, and cation concentrations between 0-4.76 mM. Fe²⁺ samples were prepared with ferrous sulfate (FeSO₄), Ca²⁺ with calcium chloride (CaCl₂), and Mg²⁺ with magnesium sulfate (MgSO₄).

Lauric acid and glycerol monolaurate vesicles with RNA captured inside (RNA-LAGML)

Figure 26 displays the absorbance readings of LAGML vesicles put through one wet-dry cycle in the presence of RNA, where absorbance readings (i.e., aggregation) increases with increasing calcium, iron, and magnesium cation concentrations.

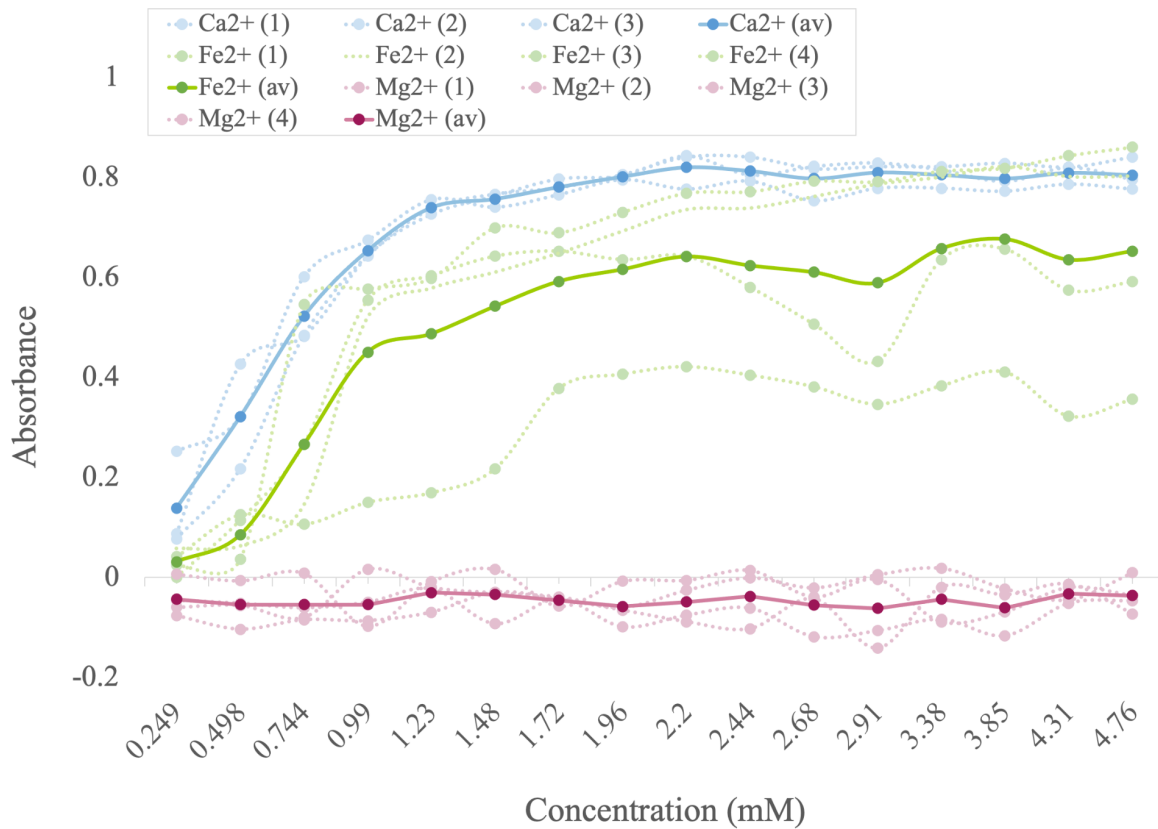


Figure 26: Light absorbance of RNA-LAGML lipid vesicle solutions with increasing cation concentrations, pH 7.5. High absorbance readings reflect high amounts of aggregation and unfavorable conditions for protocell formation. Dotted lines represent triplicate samples, solid lines represent the average of triplicates. Samples were analyzed using spectrophotometry at 400 nm under anaerobic conditions. LAGML was 10 mM in solution in a 4:1 ratio with RNA, and cation concentrations between 0-4.76 mM. Fe²⁺ samples were prepared with ferrous sulfate (FeSO₄), Ca²⁺ with calcium chloride (CaCl₂), and Mg²⁺ with magnesium sulfate (MgSO₄).

Appendix 3: Ionic compositions of hot springs vs. seawater, implications for the role of salt in protocell assembly

Salt (NaCl) has a strong osmotic effect that destabilizes lipid vesicles (as observed in Figure 27) and has been shown to prevent protocell formation (Milshteyn et al., 2018). This is a major argument for the terrestrial hot spring hypothesis as a site for the origin of life as opposed to deep-sea alkaline hydrothermal vent settings. Given the extensive evidence for salty brines on Mars (section 7.2), high concentrations of salt could have been a significant selective barrier for emerging protocell communities on Mars.

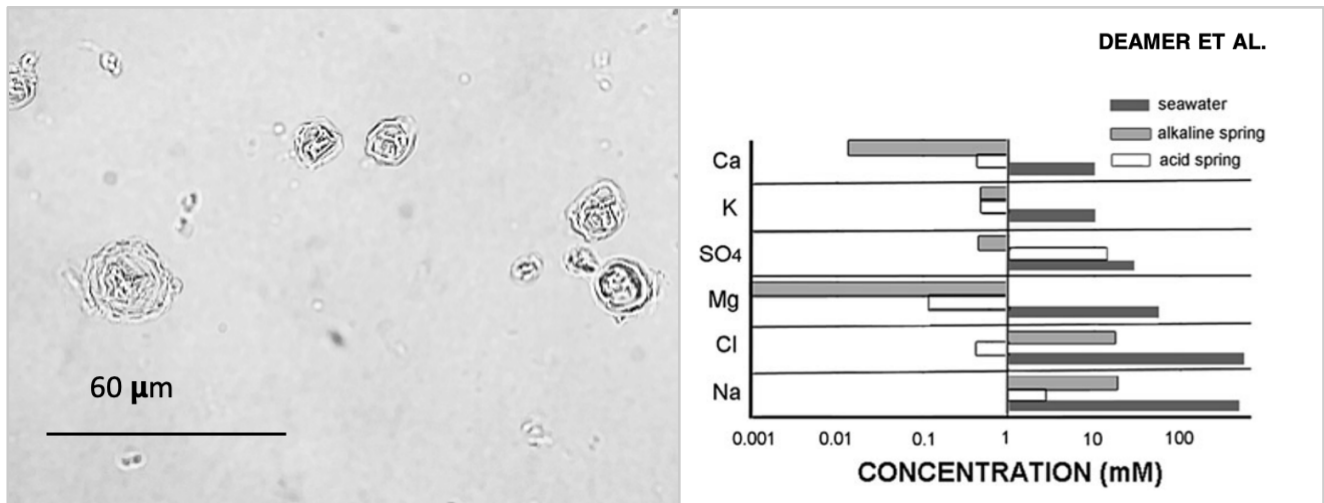


Figure 27: Panel A: LAGML vesicles immediately after exposure to salt water (NaCl₂, 30 mM). Panel B: the ionic composition of hydrothermal and seawater comparatively, taken from Deamer et al. (2019). Concentrations presented on a logarithmic scale. Alkaline and acidic hot springs from the Taupo Volcanic Zone (Rotorua, New Zealand) were included in the hydrothermal ionic composition sampling, and seawater solutions contained more than 20 times the concentration of salt and other cations than hydrothermal settings.

Appendix 4: Spectrophotometer wavelength justification

Maximum absorbance/minimum transmission was observed to be at 400 nm via spectrophotometry (Figure 28) for LAGML samples with 4.76 mM calcium, iron, and magnesium cations, the concentration where maximum aggregation was measured in this research.

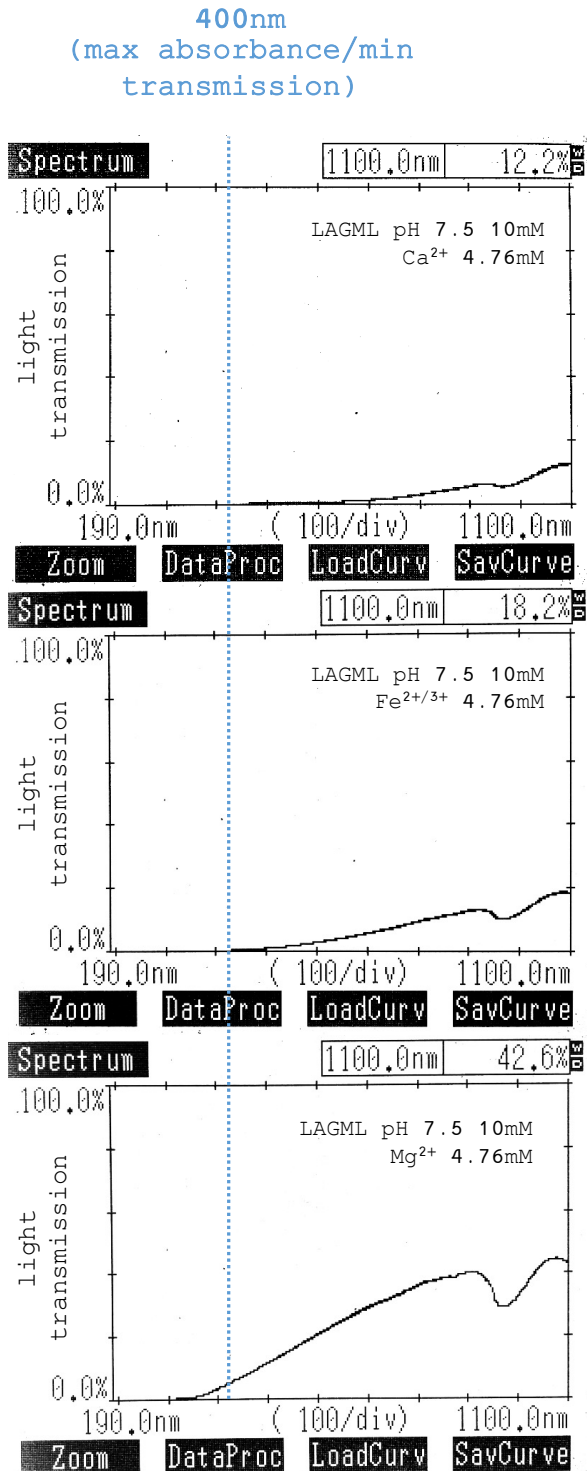


Figure 28: Spectrophotometer scans of LAGML samples containing 4.76 mM CaCl₂, FeSO₄ or MgSO₄, where maximum light transmission was ~ 400 nm.